Tutor/s

Dra. Inmaculada Angurell Purroy
Departament de Química Inorgànica i Orgànica (Secció de Química Inorgànica)

Grau de Química

Treball Final de Grau

Synthesis of luminescent gold organometallic complexes containing triphenylene ligands

Síntesi de complexos organometàl·lics d'or luminescents amb lligands de trifenilè

Xavier Bravo Serres

January 2022

Universitat de Barcelona

B:KC Barcelona Knowledge Campus
Campus d'Excel·lència Internacional

No es oro todo lo que reluce

En primer lloc, voldria agrair a la Dra. Inmaculada Angurell, tutora d'aquest treball, per supervisar aquest projecte i pel bon tracte que m'ha donat en aquests mesos, sempre enfocant positivament els obstacles amb els quals ens hem enfrontat.

A l'Andrea, per ajudar-me i compartir els seus coneixement sobre la fotoquímica. També, a l'Araceli i a la resta del grup de recerca, per tota la seva ajuda oferta ja sigués per a resoldre algun dubte, trobar un reactiu o deixar-me les claus.

A la meva família, per estar dia rere dia al meu costat i fer-me veure que un pot amb tot si s'esforça i que si un dia les coses surten malament, el següent ja aniran millor. Til familien min, glemmer jeg dere ikke og håper vi kan se hverandre snart.

A la meva parella, per recolzar-me en tot moment i fer-me suport en tots els moments d'adversitat tot i no entendre la majoria de problemes que m'ocorrien.

Sense tots vosaltres la consecució d'aquest treball de final de grau no hagués estat possible. Gràcies de tot cor.

REPORT

CONTENTS

1. SUMMARY

From the beginning of the century, there has been an increasing interest in the research of organometallic complexes with luminescent properties. Due to their wide range of applications, they can be useful as light emitting diodes, chemosensors, etc.

In this project, gold(I) luminescent complexes have been studied and synthesized. Two triphenylene (TP) based derivatives with alkynyl moieties have been used, METP and HETP, as the polycyclic aromatic hydrocarbons (PAH) ligand of the complex. On the other hand, different phosphine ligands were employed to complete the gold(I) coordination, such as PPh_3, PEt_3, PMe_3 and DAPTA.

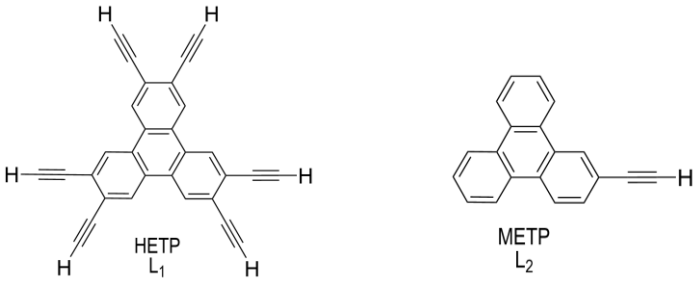

Structures of HETP and METP.

The obtained products have been characterized using the usual techniques such as ^{1}H, ^{31}P and ^{13}C NMR, HSQC, COSY, IR and mass spectrometry.

The luminescent properties of these compounds have been determined by recording the absorption and emission spectra.

Keywords: gold(I), luminescent, triphenylene, alkynyl, PAH, phosphine.

2. RESUM

Desde començament de segle, hi ha hagut un interés creixent en la recerca de complexos organometàl·lics amb propietats luminescents. Degut al seu ampli ventall d'aplicacions poden ser útils com a díodes emissors de llum, sensors químics, etc.

En aquest projecte, s'han sintetitzat i estudiat complexes d'or(I) luminescents. S'han utilitzat dos derivats del trifenilè amb fraccions d'alquinil, el METP i el HETP, com el lligand hidrocarbur aromàtic policíclic (HAP) del complex. D'altra banda per completar la coordinació de l'or(I) s'han emprat diferents lligands fosfina com la PPh_3, la PEt_3, la PMe_3 i la DAPTA.

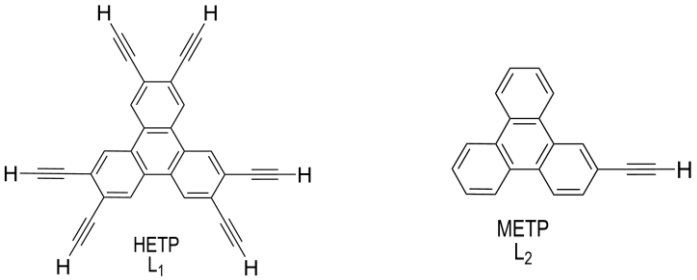

Estructures del HETP i del METP.

Els productes obtinguts s'han caracteritzat utilitzants les tècniques habituals com ^{1}H, ^{31}P i ^{13}C RMN, HSQC, COSY, IR i espectrometria de masses.

Les propietats luminescents dels compostos s'han determinat mitjançant l'enregistrament dels espectres d'absorció i d'emissió.

Paraules clau: or(I), luminescent, trifenilè, alquinil, HAP, fosfina.

3. INTRODUCTION

Over the last two decades, there has been an increasing interest in organometallic complexes with emissive properties, mainly due to their several applications such as light-emitting diodes, chemical sensors and bioimaging probes. In particular, gold(I) complexes have specially been a subject to study owing to their luminescent properties. These properties can come from both the nature of the ligands and the aurophilic interactions, either intra- or intermolecular, which occur between two gold atoms[1]. Gold(I) is a closed-shell cation with an electronic configuration of $5d^{10}6s^{0}$, which causes the certain stability of gold(I) complexes and makes d-d transitions not possible[2].

The term luminescence refers to the emission in the range from the infrared light to the ultraviolet, going through the optical visible, after one or another form of energy has been transferred to the molecule. To be more precise, this emission must continue after the excitation energy has been absorbed for a time that is significantly longer than the period of the light waves[3]. Luminescence is inherent in substances in any aggregate state and different types of luminescence exists contingent on the method substance excitation. These can be photoluminescence (light), radioluminescence (ionizing radiation), thermoluminescence (preirradiation and heat), chemiluminescence (chemical reactions), triboluminescence (mechanical influences) and sonoluminescence (ultrasounds).

Fluorescence and phosphorescence are the two most studied forms of photoluminescence. The first phenomenon is a radiation that quickly decays after the excitation stops, due to the transition from the lowest vibrational level of the lowest singlet excited state to the lowest vibrational level of the ground singlet state (figure 1). The average time of duration of fluorescence is of the order of 10^{-8} s. On the other hand, phosphorescence occurs due to the radiative transition from the lowest triplet state to the ground singlet state (figure 1). This phenomenon is preceded by an intersystem crossing (ISC), which induces a transition from an excited singlet state to an excited triplet state lower in energy. The duration of phosphorescence is longer than fluorescence because of the spin forbideness of the transition, going from 10^{-5} s up to some hours[4].

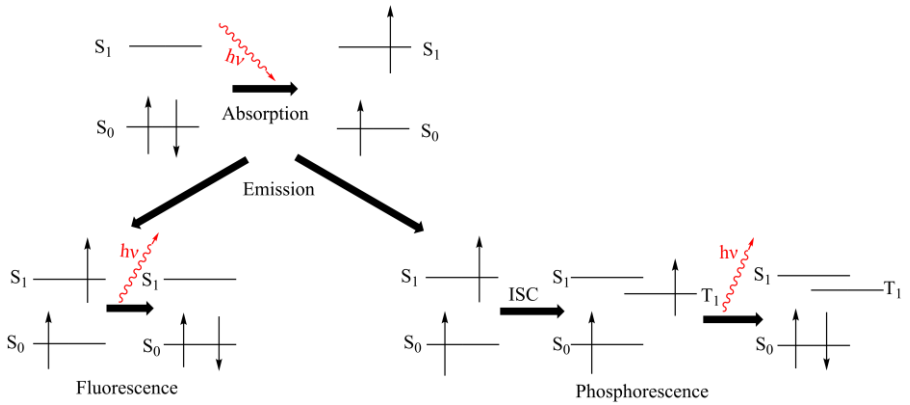

Figure 1. Fluorescence and Phosphorescence representation.

As was mentioned earlier, the aurophilic interaction plays a crucial role to the photophysical properties of gold(I) complexes. The heavy atom and the formation of aggregates, enhance spin-orbit coupling (SOC) that relaxes the spin selection rule, allowing a fast rate of ISC and favors the phosphorescence[5,6]. This metallophilic bond has a length of approximately 3.0 Å and its energy is estimated to be between 5 and 10 kcal/mol, which is comparable to the strength of a standard hydrogen bond[1]. Although, a repulsion between two gold cations should be expected, due to relativistic effects, aurophilic interaction do exist. Particularly, on average, 28% of the binding energy in the aurophilic interaction can be assigned to relativistic expansion of the gold d orbitals[7]. The linear coordination of Au(I) atoms favors these aurophilic contacts. Regarding this, the two ligands occupying the coordination positions will have a straight influence on the establishment of aurophilic interactions and determine the structure of the resulting possible intra- or intermolecular assemblies and its corresponding luminescence[8]. The solubility also can affect aurophilic interactions, being able to display intrinsic aggregation induced emission (AIE) at low solubility conditions[8].

In recent years, the attention put to flat polycyclic aromatic hydrocarbons (PAH) has increased, because of their characteristic structural and electronic properties for extended π-conjugation. Triphenylene is one of these type of compounds due to its high absorption coefficient, fluorescence quantum yield, and photostability. The aromacity of a PAH can be extended by the addition of an alkynyl moiety at one or more brominated positions via Sonogashira coupling[6]. Despite recent studies that confront the use of the term π-stacking or π-π interactions and suggest the term's lack of precision in some cases[9], it does exist an

intermolecular aromatic interaction between the aromatic rings of flat PAHs that enhances the stability of the compounds.

The Hunter and Sanders model, sometimes referred as polar/pi considerations, states that pi electron density on most aromatic rings implies a quadrupole moment with partial negative charge above both aromatic faces and a partial positive charge on the edges. Two quadrupole moments like these in proximity should avoid face-centred parallel stacking in favour of perpendicular edge-to-face interactions or off-centred parallel stacking. On the other hand, this model notes that the situation is completely different when one member of an aromatic pair possesses strongly electron-withdrawing groups and the other one contains electron-donating groups. This change in the resulting quadrupole moment implies a change on the geometry and favours a face-centred pairing. These aromatic interactions are shown in figure 2.

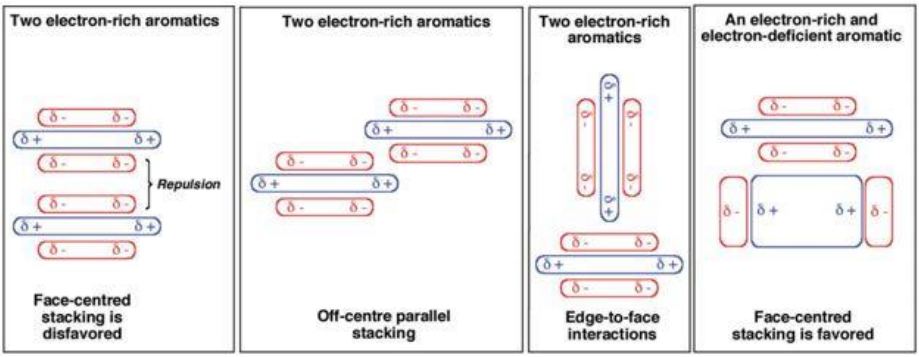

Figure 2. Aromatic interactions between PAHs *(image extracted from Martinez, ref. 9)*.

As it was mentioned earlier, an alkynyl moiety extends the aromaticity of a PAH, which makes, among gold(I) complexes, alkynyl derivatives interesting to study in conjunction with the preference of gold(I) for a two-linear coordination geometry and with the linearity of an acetylide and its π-unsaturated nature. These compounds establish M-π (C≡C) interactions, which can induce or modify the luminescent properties of these molecules. The emission found in these compounds is attributed to the π→π*-(C≡C) or π→π*-(C≡C-R) transitions[8,10].

The second coordination position is usually occupied by phosphanes, since they have the ability of modulate the solubility in different solvents. These complexes containing phosphanes exhibit emission bands that are assigned to σ-(Au-P)→π*(C≡C) or σ-(Au-P)→π*(C≡C-R) transitions[11].

In this work, it has been synthesized an organic ligand with alkynyl moieties starting from triphenylene. Triphenylene is a PAH that consists in four fused benzene rings. It has 18 π electrons delocalized on a planar structure, which implies an extended π-conjugation. With this ligand gold(I) luminescent complexes are achieved and ready to be studied.

4. OBJECTIVES

The first objective will be the synthesis of a PAH alkynyl ligand. The starting point will be triphenylene and going through a three-step synthetic pathway, hexa-ethynyl-triphenylene (HETP) will be obtained.

The second objective will be to coordinate this ligand together with different gold(I) phosphine complexes. Gold complexes with the equivalent ligand with one just alkynyl moiety, known as mono-ethynyl-triphenylene (METP), will also be made. The phosphines used will be triphenylphosphine (PPh_3), triethylphosphine (PEt_3), trimethylphosphine (PMe_3), 1,1'-(1,3,7-Triaza-5-phosphabicyclo[3.3.1]nonane-3,7-diyl)diethanone (DAPTA).

The final goal of this work will be to study and compare the luminescent properties of these complexes recording its absorption and emission spectra. The structures of HETP and METP are shown in figure 3.

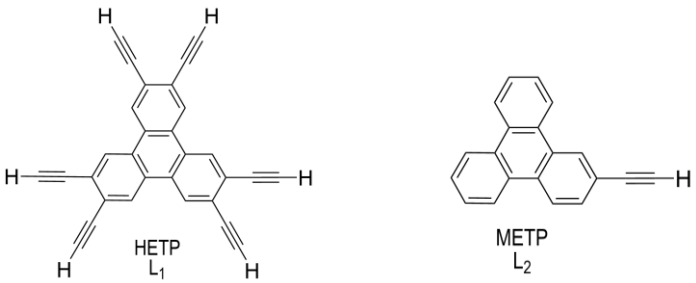

Figure 3. Structures of HETP and METP.

5. EXPERIMENTAL SECTION

Firstly, a description of the methods and the instrumentation used for the preparation of all compounds is shown in this section. Secondly, a detailed synthesis of the complexes prepared and its characterization can be found in the second part of this section.

5.1. METHODS AND INSTRUMENTATION

5.1.1. Nuclear magnetic resonance (NMR) ^{1}H, $^{31}P\{^{1}H\}$, $^{13}C\{^{1}H\}$, COSY and HSQC

^{1}H NMR spectra were recorded at room temperature (25°C) using a Varian Mercury 400 Spectrometer or a Bruker 400 Spectrometer. Chemical shifts (δ) are shown in ppm and are referenced to intern deuterated chloroform ($CDCl_3$), 7.26 ppm for ^{1}H NMR. The data are reported as follows: chemical shift (multiplicity, coupling constant *J* (if necessary), number of protons, type of proton); multiplicity is noted as follows: s, for singlet; d, for doublet; t, for triplet; q, for quartet; m, for multiplet; dd, for doublet of doublets, br. for broad. The coupling constants, *J*, are quoted in Hz. In the case of the presence of more than one coupling constant for a peak, the larger coupling constant is shown first and the smaller one is shown afterwards. The solvent and the frequency used are described in each characterization.

$^{31}P\{^{1}H\}$ NMR spectra (from now on just referred as ^{31}P NMR) were recorded at room temperature (25°C) using a Bruker 400 or 500 Spectrometer. Chemical shifts (δ) are shown in ppm and the data are reported as follows: chemical shift (related compound, proportion (if needed)). The solvent and the frequency used are described in each characterization.

$^{13}C\{^{1}H\}$ NMR spectra (from now on just referred as ^{13}C NMR) were recorded at room temperature (25°C) using a Varian Mercury 400 Spectrometer. Chemical shifts (δ) are shown in ppm and referenced to intern deuterated chloroform ($CDCl_3$), 77.16 ppm for ^{13}C NMR. The data are reported as follows: chemical shift (multiplicity, coupling constants, *J* (if necessary), type of carbon). The multiplicity is noted equally as ^{1}H NMR and the coupling constants, *J*, are quoted in Hz in the same way as ^{1}H NMR ones. The solvent and the frequency used are described in each characterization.

The 2D spectra that have been used to characterize some compounds are COSY and HSQC. The spectra were recorded at room temperature (25°C) using a Bruker 400 Spectrometer.

5.1.2. Infrared spectroscopy (IR)

IR spectra (Attenuated Total Reflectance, ATR) were recorded at room temperature using a Nicolet iS5 FT-IR Thermo Scientific Spectrometer. The wavenumbers are reported in cm^{-1} and only the most important peaks are quoted. The data are reported as follows: wavenumber (type of vibration). The acronyms used are the following ones: st. for *stretching*, be. for *bending*, ov. for *overtone* and op. for *out of plane*.

5.1.3. Mass spectrometry

Mass spectrometry were recorded at room temperature using either a Fisons VG Quatro spectrometer for ElectroSpray spectra (+) or a Applied Biosystems 4700 Proteomics Analyzer for MALDI-TOF spectra (+). The data are reported as follows: (technique used), m/z calc. for [fragment] *mass*, found *mass*.

5.1.4. Thin-Layer Chromatography (TLC)

TLC were carried out on Merck Silica gel 60 F_{254} (0.2 mm thickness) and analyzed with 254 nm ultraviolet light (UV) mainly as well as 312 and 400 nm. The mobile phase is specified in each case.

5.1.5. Column Chromatography

This technique was used in order to purify substances. Silica gel was used as stationary phase and the eluent is defined in each case.

5.1.6. Luminescence Spectra

The absorption spectra were recorded on a Varian Cary 100 Bio UV-spectrophotometer and emission spectra on a Horiba-Jobin-Yvon SPEX Nanolog spectrofluorometer.

5.2. SYNTHESES

5.2.1. Synthesis of 2,3,6,7,10,11-hexabromotriphenylene

20.2 mg of Fe (0.362 mmol) powder and 200 mg of triphenylene (0.876 mmol) (TP) were added into 20 mL of degassed nitrobenzene. The mixture was kept under nitrogen atmosphere and stirred for 10 minutes. Then, 1 mL of liquid bromine (Br_2) was added and the system was heated up to 100°C. Once the temperature was reached, the mixture is heated slowly up to 160°C while stirring for 2 hours. The mixture was quenched with 50 mL of diethyl ether and a white powder was obtained. The precipitate was filtrated and washed three times with diethyl ether, filtrated with a cannula and dried under vacuum to yield 2,3,6,7,10,11-hexabromotriphenylene (HBTP) as a white powder.

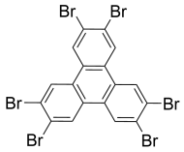

White powder; HRMS (MALDI), m/z calc. for $[M]^+$ 701.55, found 701.5; m/z calc. for $[M\text{-}HBr]^+$ 621.62, found 621.6.

5.2.2. Synthesis of 2,3,6,7,10,11-hexa(trimethylsilylethynyl)triphenylene

614 mg of HBTP (0.876 mmol), 495 mg of $[PdCl_2(PPh_3)_2]$ (0.705 mmol), 267 mg of CuI (1.40 mmol) and 371 mg of PPh_3 (1.42 mmol) were added into 60 mL of a solution of triethylamine and toluene (v/v) (1:1). The mixture was stirred for 10 minutes at room temperature before 1.2 mL of trimethylsilylacetylene (TMS-C≡CH) (8.67 mmol) was added to the suspension. Next, the mixture was stirred under nitrogen atmosphere at 80°C, overnight. On the next day, the mixture was dried under vacuum with an auxiliary trap. Once the product was well dried, it was purified with a silica gel column chromatography with ethyl acetate, and dried under vacuum. The raw residue was analyzed by ^1H NMR.

The raw product was purified by column chromatography using as eluent a mixture of hexane and dichloromethane (DCM) (v/v) (5:1). The fractions were analyzed by TLC and ^1H NMR, gathered the pure ones (Rf: 0.13) and dried under vacuum to yield 542 mg of a yellow powder of hexa(trimethylsilylethynyl)triphenylene (HTMSTP). (Yield of the first two reactions: 77%).

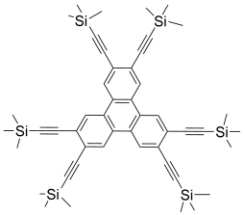

Yellow powder: IR: 2958+2898 (st. Csp^3-H), 2158 (st. C≡C), 1555+1482 (st. C=C Ar). ^{1}H NMR ($CDCl_3$, 400 MHz) δ: 8.65 (s, 6H, CH Ar), 0.35 (s, 54H, CH_3).

5.2.3. Synthesis of 2,3,6,7,10,11-hexaethynyltriphenylene

542 mg of HTMSTP (0.674 mmol) were dissolved in 16 mL of tetrahydrofuran (THF), then, 5.2 mL of tetrabutylammonium fluoride (TBAF) (1 M TBAF in THF, 5.2 mmol) were added to the previous solution and stirred at room temperature under nitrogen atmosphere for an hour. The mixture was diluted with 50 mL of DCM, washed three times with distilled water and dried with anhydrous $MgSO_4$. Finally, the solvent was removed under vacuum to yield raw product 2,3,6,7,10,11-hexaethynyltriphenylene (HETP). The raw product was analyzed by ^{1}H NMR.

The raw product was recrystallized in methanol and a cannula filtration was done. The purified product was also characterized by ^{1}H NMR. 0.225 g of a brown powder HETP were obtained. (Yield: 90%).

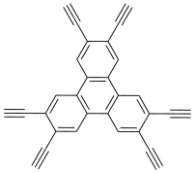

Brown powder; IR: 3274 (st. Csp-H), 2109 (st. C≡C), 1602+1484 (st. C=C Ar). ^{1}H NMR ($CDCl_3$, 400 MHz) δ: 8.70 (s, 6H, CH Ar), 3.50 (s, 6H, HC≡C).

5.2.4. Synthesis of [METP-Au-PPh_3]

20.1 mg of 2-ethynyl-triphenylene (METP) (0.0797 mmol) were dissolved in 11 mL of MeOH and stirred together with 7.80 mg of KOH (0.139 mmol) for 1 hour at room temperature. Then, 41.7 mg of [AuCl(PPh_3)] (0.0843 mmol) were added and the resulting mixture was allowed to stir for 48 hours. Past that time, the solution was filtrated by cannula and the solid was dried under vacuum. Finally, the product was characterized by IR, ^{1}H NMR, ^{31}P NMR and mass spectrometry and 39.2 mg (0.0552 mmol) of a bright yellow powder were obtained. (Yield: 70%).

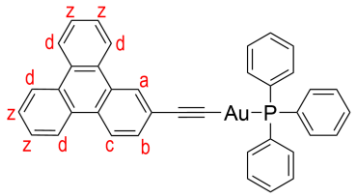

Bright yellow powder; IR: 3075 (st. Csp^2-H), 2155 (st. C≡C), 1605+1479 (st. C=C Ar), 749 (be. =C-H op.). ^{1}H NMR ($CDCl_3$, 500 MHz) δ: 8.84 (d, J=1.5, 1H, CH Ar *a*), 8.65-8.59 (m, 4H, CH Ar *d*), 8.54 (d, J=8.6, 1H, CH Ar *c*), 7.80-7.78 (dd, J_1=8.5, J_2=1.6, 1H, CH Ar *b*), 7.65-7.45 (m, 15H, Ph_3), 7.65-7.45 (m, 4H, CH Ar *z*). ^{31}P NMR ($CDCl_3$, 202 MHz) δ: 42.3 ([METP-Au-PPh_3], maj.), 33.2 ([AuCl(PPh_3)], min.). HRMS (ESI), m/z calc. for $[2M\text{-}METP]^+$ 1169.20, found 1169.20; m/z calc. for $[Au(PPh_3)_2]^+$ 721.15, found 721.15.

5.2.5. Synthesis of [METP-Au-PEt_3]

20.0 mg of METP (0.0793 mmol) were dissolved in 12 mL of MeOH in conjunction with 7.80 mg of KOH (0.139 mmol) and were stirred for 1 hour at room temperature. After this time, 29.2 mg of [AuCl(PEt_3)] (0.0833 mmol) were added and the solution was stirred overnight. On the next day, the mixture was filtrated by cannula and the crude was dried under vacuum, yielding 30.6 mg (0.0540 mmol) of a bright yellow powder. Lastly, the product was analyzed by IR, ^{1}H NMR, ^{31}P NMR and mass spectrometry. (Yield: 68%).

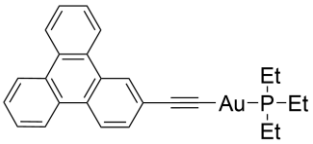

Bright yellow powder; IR: 3069 (st. Csp^2-H), 2966+2929 (st. Csp^3-H), 2116 (st. C≡C), 1605+1488 (st. C=C Ar), 1449 (be. CH_2), 1379 (be. CH_3), 759 (be. =C-H op.). ^{1}H NMR ($CDCl_3$, 500 MHz) δ: 8.81 (s, 1H, CH Ar *a*), 8.72-8.57 (m, 4H, CH Ar *d*), 8.52 ("d", 1H, CH Ar *c*), 7.76 ("dd", 1H, CH Ar *b*), 7.70-7.55 (m, 4H, CH Ar *z*), 1.84 (br. s, 6H, P-$\underline{CH_2}$-CH_3), 1.24 (br. s, 9H, P-CH_2-$\underline{CH_3}$). ^{31}P NMR ($CDCl_3$, 202 MHz) δ: 38.1 [METP-Au-PEt_3]. HRMS (ESI), m/z calc. for $[M+H]^+$ 567.15, found 567.15; m/z calc. for $[M+Na]^+$ 589.13, found 589.14; m/z calc. for $[2M\text{-}METP]^+$ 881.20, found 881.20.

5.2.6. Synthesis of [METP-Au-PMe_3]

20.0 mg of METP (0.0793 mmol) were dissolved in 12 mL of MeOH together with 14.8 mg of KOH (0.263 mmol) and were stirred during 1 hour at room temperature. Then, 25.8 mg of [AuCl(PMe_3)] (0.0836 mmol) were added and the suspension was allowed to stir overnight. On the next day, the mixture was cannula filtrated and the solid was dried under vacuum. The solid was recrystallized using DCM and hexane. Afterwards, it was cannula filtrated and dried under vacuum yielding 29.7 mg (0.0567 mmol) of an orange/brown powder. The solid was analyzed by IR, ^{1}H NMR and ^{31}P NMR. (Yield: 71%).

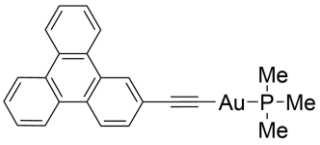

Lemon yellow powder; IR: 3084 (st. Csp^2-H), 2965 (st. Csp^3-H), 2113 (st. C≡C), 1604+1487 (st. C=C Ar), 1398 (be. CH_3), 752 (be. =C-H op.). ^{1}H NMR ($CDCl_3$, 400 MHz) δ: 8.82 (s, 1H, CH Ar *a*), 8.68-8.58 (m, 4H, CH Ar *d*), 8.52 ("d", 1H, CH Ar *c*), 7.75 (d, J=8.3, 1H, CH Ar *b*), 7.70-7.62 (m, 4H, CH Ar *z*), 1.57 (d, J=10.7, 9H, P-CH_3). ^{31}P NMR (dmso, 202 MHz) δ: 1.2 ([METP-Au-PMe_3], maj.), -10.3 ([AuCl(PMe_3)], min.).

5.2.7. Synthesis of [METP-Au-DAPTA]

7.60 mg of METP (0.0301 mmol) were dissolved in 12 mL of MeOH together with 13.1 mg of KOH (0.234 mmol) and the solution was stirred 1 hour at room temperature. Past that time, 14.9 mg of [AuCl(DAPTA)] were added and the mixture was allowed to stir overnight. On the next day, the mixture was filtrated by cannula and the solid was dried under vacuum; yielding 16.5 mg (0.0244 mmol) of a light yellow powder. The product was characterized by IR, ^{1}H NMR, ^{31}P NMR, ^{13}C NMR, COSY, HSQC and mass spectrometry. (Yield: 81%).

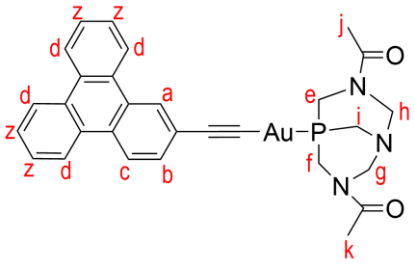

Light yellow powder; IR: 3430 (ov. C=O), 3051 (st. Csp^2-H), 2923 (st. Csp^3-H), 2056 (st. C≡C), 1637 (st. C=O), 1370 (be. CH_3), 755 (be. =C-H op.). ^{1}H NMR ($CDCl_3$, 400 MHz) δ: 8.79 (s, 1H, CH Ar *a*), 8.64-8.57 (m, 4H CH Ar *d*), 8.54 (d, J=8.6, 1H, CH Ar *c*), 7.73 (d, J=8.3, 1H, CH Ar *b*), 7.67-7.62 (m, 4H, CH Ar *z*), 5.78 (d, J=14.4, 1H, H*g*), 5.67 (dd, J_1=15.9, J_2=7.2, 1H, H*e*), 4.93 (d, J=14.0, 1H, H*h*), 4.69 (dd, 1H, H*f*), 4.63 (d, J=14.5, 1H, H*h'*), 4.18 (dd, J_1=15.5, 1H, H*f'*), 4.05 (d, J=14.4, 1H, H*g'*), 3.9 (s, 2H, H*i*), 3.62 (dd, J_1=13.1, 1H, H*e'*), 2.11-2.10 (s+s, 3H+3H, CH_3*j*/CH_3*k*). ^{13}C NMR ($CDCl_3$, 100 MHz) δ: 170.2-170 (s+s, C=O), 130.1 (s, C*b*), 127.5 (s, C*a*), 127.4 (s, C*z*), 123.6 (s, C*d*), 123.5 (s, C*c*), 67.5 (s, C*h*), 62.3 (s, C*g*), 49.6 (d, J=25.9, C*i*), 45 (d, J=26.2, C*f*), 39.8 (d, J=27.2, C*e*), 21.7-21.4 (s+s, C*j*/C*k*). ^{31}P NMR ($CDCl_3$, 202 MHz) δ: 1.53 (min.), -22.1 (maj.), [METP-Au-DAPTA]. HRMS (ESI), m/z calc. for $[DAPTA+H]^+$ 230.11, found 230.11; m/z calc. for $[DAPTA+Na]^+$ 252.09, found 252.09.

5.2.8. Synthesis of [HETP-(Au-PPh_3)$_6$]

15.1 mg of HETP (0.0406 mmol) were dissolved in 16 mL of MeOH and the solution was stirred for 10 minutes. Then, 27.6 mg of KOH (0.492 mmol) were added and the mixture was

heated at reflux (75°C) under nitrogen atmosphere for 3 hours. After that, the mixture was allowed to cold at room temperature, and then, 126 mg of [AuCl(PPh_3)] (0.255 mmol) were added and it was stirred overnight while heated at 35°C. On the next day, DCM was added and the mixture was filtrated by cannula. The crude was dried under vacuum yielding 81.7 mg (0.0262 mmol) of an orange/brown powder. Finally, the product was characterized by IR, ^{1}H NMR, ^{31}P NMR and mass spectrometry. (Yield: 65%).

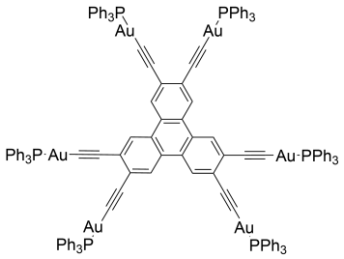

Orange/brown powder; IR: 3056 (st. Csp^2-H), 2163 (st. C≡C), 1570+1479 (st. C=C Ar), 747 (be. =C-H op.). ^{1}H NMR ($CDCl_3$, 400 MHZ) δ: 8.71 (s, 6H, CH Ar), 7.56-7.45 (m, 90H, PPh_3). ^{31}P NMR ($CDCl_3$, 162 MHz) δ: 42.1 [HETP-(Au-PPh_3)$_6$], 33.2 [AuCl(PPh_3)]. HRMS (MALDI), m/z calc. for [Au(PPh_3)$_2$] 721.15, found 721.15.

5.2.9. Synthesis of [HETP-(Au-PEt_3)$_6$]

15.1 mg of HETP (0.0406 mmol) were dissolved with 12 mL of MeOH in a schlenk. Then, 29.7 mg of KOH (0.529 mmol) were added to the mixture and it was heated at reflux for 3 hours. To continue, 89.7 mg of [AuCl(PEt_3)] (0.256 mmol) were added and the solution was stirred overnight at room temperature. On the next day, some KOH was added along with 10 mL of DCM, and the mixture was allowed to stir over the weekend. After these days, the mixture was filtrated through cannula and dried under vacuum. The solid and filtrate was characterized by IR, ^{1}H NMR and ^{31}P NMR. (Yield: 42%).

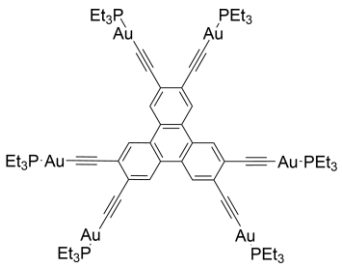

Light brown powder; IR: 3099 (st. Csp^2-H), 2959 (st. Csp^3-H), 1488 (be. CH_2), 1377 (be. CH_3). ^{1}H NMR (dmso, 400 MHz) δ: 8.78 (s, 6H, CH Ar), 1.98-1.88 (dq, J_1=10.7, J_2=7.7, P-$\underline{CH_2}$-CH_3), 1.13-1.05 (dt, J_1=19.0, J_2=7.6, 9H, P-CH_2-$\underline{CH_3}$). ^{31}P NMR (dmso, 162 MHz) δ: 33.9 [HETP-(Au-PEt_3)$_6$]. HRMS (MALDI), m/z calc. for [M+H]$^+$ 2257.40, found 2259.20; m/z calc. for [M-(AuPEt_3)+H]$^+$ 1942.34, found 1945.20; m/z calc. for [M-(2AuPEt_3)+H]$^+$ 1627.28, found 1629.20; m/z calc. for [M-(3AuPEt_3)+H]$^+$ 1312.22, found 1315.20.

5.2.10. Synthesis of [HETP-(Au-DAPTA)$_6$]

5.00 mg of HETP (0.0135 mmol) were dissolved in 12 mL of MeOH along with 11.9 mg of KOH (0.212 mmol) and the solution was stirred for 3 hours and heated at reflux at 75°C. Afterwards, the mixture was allowed to cold at room temperature. Then, 39.2 mg of [AuCl(DAPTA)] (0.0849 mmol) were added and the mixture was stirred overnight at room temperature. The day after, the mixture was cannula filtrated and dried under vacuum the crude, yielding 34.4 mg (0.0117 mmol) of a yellow/light brown powder. The product was characterized by IR, ^{1}H NMR, ^{31}P NMR and mass spectrometry. (Yield: 87%).

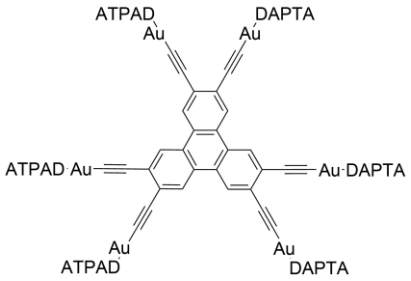

Yellow/light brown powder; IR: 3427 (ov. C=O), 2959+2923 (st. Csp^3-H), 2110 (st. C≡C), 1633 (st. C=O), 1412 (be. CH_2), 1331 (be. CH_3), 791 (be. =C-H op.). ^{1}H NMR ($CDCl_3$, 400 MHz) δ: 8.72 (s, 6H, CH Ar), 5.81 (d, J=17.1, 1H, H*g*), 5.69 (dd, J_1=16.4, J_2=7.4, 1H, H*e*), 4.98 (d, J=13.2, 1H, H*h*), 4.70-4.63 (dd, 1H, H*f*), 4.70-4.63 (d, 1H, H*h'*), 4.15-4.06 (dd, 1H, H*f'*), 4.15-4.06 (d, 1H, H*g'*), 3.86 (s, 2H, H*i*), 3.63 (dd, 1H, H*e'*), 2.12 (s, 6H, CH_3*j*/CH_3*k*). ^{31}P NMR ($CDCl_3$, 162 MHz) δ: 1.5, -34.0 [HETP-(Au-DAPTA)$_6$].

6. RESULTS AND DISCUSSION

6.1. SYNTHESES AND CHARACTERIZATION

6.1.1. Synthesis of HETP

As it was commented before one of the aims of this project was to study the luminescent properties of triphenylene-based gold(I) complexes. To improve these properties, it was necessary to extend the conjugation of triphenylene and it was done by adding alkynyl moieties. Three steps had to be made to yield the final ligand HETP according to the literature[12]. It included a bromination reaction, followed by a Sonogashira coupling and a final deprotection of the tetramethylsilane (TMS) as it can be seen in scheme 1.

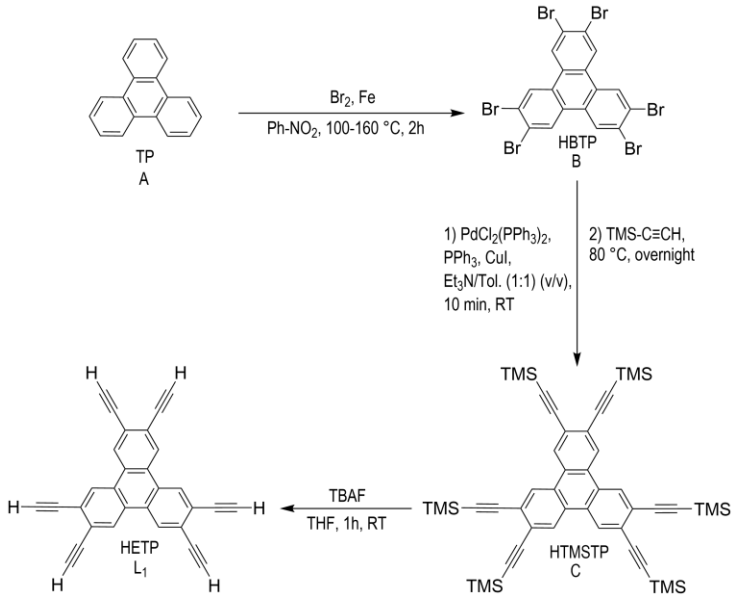

Scheme 1. Synthesis of HETP.

The first step consisted on a bromination of triphenylene using degassed nitrobenzene as a solvent and iron as a catalyst. The literature stirs the mixture at 160°C for 2 hours, whereas we heated the mixture first at 100°C and slowly the temperature was raised up to 160°C due to the volatility of the liquid bromine. The mixture was quenched and washed with diethyl ether to yield a white powder. The molecular weight of HBTP was determined through MALDI-TOF-MS, indication the successful bromination reaction.

The second step was a Sonogashira cross-coupling reaction. This type of reaction follows a catalytic cycle, with Pd(0) as a catalyst, although it is often used a Pd(II) complex as a precatalyst due to the less reactivity of the complex compared to Pd(0) and they can be stored for a longer period. A common complex of Pd(II) is $[PdCl_2(PPh_3)_2]$. The Pd(0) are obtained in situ through the losing of 2 chlorides from $[PdCl_2(PPh_3)_2]$ and the reduction of Pd(II) to Pd(0). Moreover, the CuI acts as a co-catalyst of the reaction, interacting with TMS-C≡CH. The mechanism of the catalytic cycle consists of 4 steps, which are described in figure 4.

The first step of the cycle follows an oxidative addition of the aryl bromide (HBTP in our case) to the Pd(0) catalyst. The Pd(0) specie is oxidized to Pd(II) with the addition of the aryl bromide establishing a 16-electron square planar complex. The next step of the cycle is the

trasnmetallation, where the TMS-C≡CH replace the bromide atom of the palladium complex. There is also a side-reaction where the co-catalyst CuI enhances the reactivity of TMS-C≡CH via a co-catalytic cycle. The last step of the Sonogashira cross-coupling reaction is a reductive elimination where the aryl and the trimethylsilylacetylene are extracted from the palladium complex to form the HTMSTP. On the other hand, the palladium(II) complex is reduced to the initial Pd(0) complex to start the cycle again. For this to occur, there must be a previous trans/cis isomerization process where the acetylene ligand and the aryl ligand must find each other in a cis geometry in order to take place the reductive elimination[13].

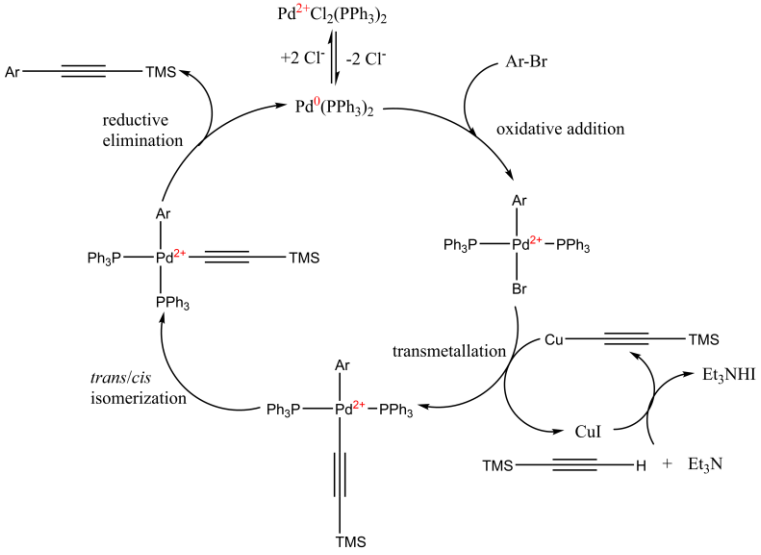

Figure 4. Sonogashira cross-coupling mechanism.

To ensure the purity of the product, the obtained HTMSTP was firstly purified using a chromatography column with AcOEt and secondly with a solution of hexane/DCM (5:1) (v/v), where the solid was collected into different fractions and analyzed through TLC. The pure ones (Rf:0.13) were gathered together and dried under vacuum yielding the purified HTMSTP. The structure of HTMSTP was confirmed by IR and ^{1}H NMR, where it could be observed the peaks of ν(C≡C) at 2150 cm^{-1} and Csp^3-H at 2958 and 2898 cm^{-1} at IR, alongside the signal of Si-Me$_3$ group at 0.35 ppm in the ^{1}H NMR.

The last step of the synthesis was the deprotection of TMS. The HTMSTP was dissolved in THF and a solution of TBAF in THF was used to deprotect the TMS. The mixture was stirred for an hour to ensure a quantitative deprotection. Then, the mixture was diluted with DCM, washed three times with distilled water and dried both with $MgSO_4$ and under vacuum. The crude was recrystallized with MeOH and, thus, HETP was obtained. The structure of HETP was analyzed by IR and ^1H NMR. The absence of the Csp^3-H peaks and the appearance of a Csp-H peak at 3274 cm^{-1} at IR together with an alkyne signal at ^1H NMR (at 3.50 ppm), ensured the correct deprotection of the HTMSTP along with the absence in ^1H NMR of signal of alkylic protons at 0.35 ppm. In figure 5 it can be seen the comparison between the ^1H NMR spectra. Moreover, it can be noticed that the aromatic protons were slightly left-shifted with the deprotection.

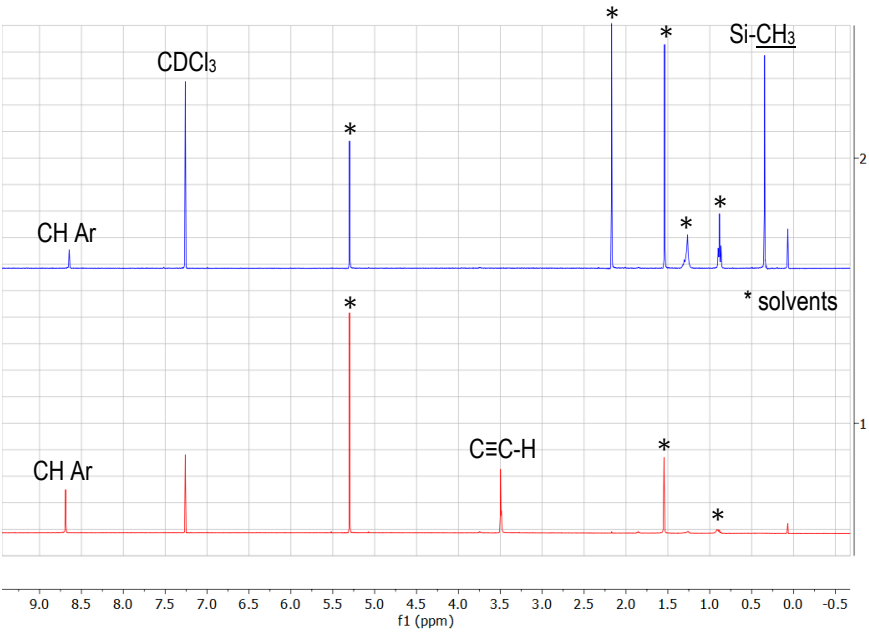

Figure 5. ^1H NMR (in $CDCl_3$) spectra of HTMSTP (up) and HETP (down) stacked.

6.1.2. Synthesis of gold(I) phosphine complexes

To be able to make the gold(I) complexes both with METP and HETP, it was required to prepare some gold(I) phosphine complexes in order to have enough amount of reactants. To prepare these precursor complexes, a synthetic path previously used by our group was

followed. In this path, a gold complex with a more labile ligand than the phosphines, as tetrahydrothiophene (tht) is, was used. The reaction consisted of an exchange of the tht with the phosphine desired as it can be seen in scheme 2. First, the complex [AuCl(tht)] was dissolved in DCM and then, the phosphine was added. The mixture was stirred for an hour at room temperature before it was dried under vacuum almost to dryness. Finally, hexane was added and the mixture was dried under vacuum to reach the wanted gold(I) phosphine complex. Later on, these phosphine gold complexes will exchange the chloride with either METP or HETP.

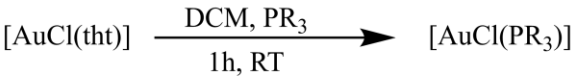

Scheme 2. Synthesis of gold(I) phosphine complexes.

6.1.3. Synthesis of METP derivatives

Due to the complexity with HETP derivatives that our group has previously noticed, it was decided to start with METP derivatives, to later on, extrapolate the results and try the syntheses with HETP-Au complexes.

Thus, the first synthesis that was tried to accomplish was the [METP-Au-PPh_3]. Following the synthetic method that our group tried before, the METP was dissolved in MeOH and deprotonated with excess of NaOH (2 eq.) at room temperature for an hour. Then, 1 eq. of [AuCl(PPh_3)] dissolved in DCM, was added and the mixture was stirred overnight. On the next day, the mixture was dried under vacuum almost to dryness and diethyl ether was added to quench the reaction, but the crude became more soluble instead. With this fact, the solution was filtrated through cannula and dried under vacuum. The product and the organic ligand were characterized by ^{1}H NMR to compare them. Looking to both spectra, it could be appreciated that the [METP-Au-PPh_3] still had the alkyne signal that the ligand has at 3.23 ppm, so it indicated that the deprotonation was not fully accomplished. A recrystallization using DCM and hexane was tried with no significant improvements.

For this reason, it was decided to repeat the reaction using KOH instead of NaOH, due to the less hygroscopicity of KOH, and adding a bit of excess of the gold complex (1.05 eq.). Doing so, a pale yellow powder of [METP-Au-PPh_3] was yielded and it was characterized through IR, ^{1}H NMR, ^{31}P NMR and mass spectrometry. Analyzing the spectra, it could be observed that the Csp-H peak at 3281 cm^{-1} of the IR was not visible anymore and it appeared the typical stretching peaks of PPh_3 at 1479 and 1435 cm^{-1}. The alkyne signal at 3.23 ppm was also almost disappeared at ^{1}H NMR, as it can be seen in figure 6. Moreover, at the ^{31}P NMR spectrum, the signal at 42.3 ppm confirmed the structure of the compound. In addition, the aromatic protons *a* and *b* were left-shifted, whereas, the aromatic proton *c* was right-shifted with the addition of the gold complex to the ligand. The remaining protons *d* and *z* were not affected. Finally, the mass spectrum did not reveal any significant information as the fragments found were the [2M-METP]$^+$ and [AuCl(PPh_3)]$^+$, being this last one very common among triphenylphosphine gold complexes.

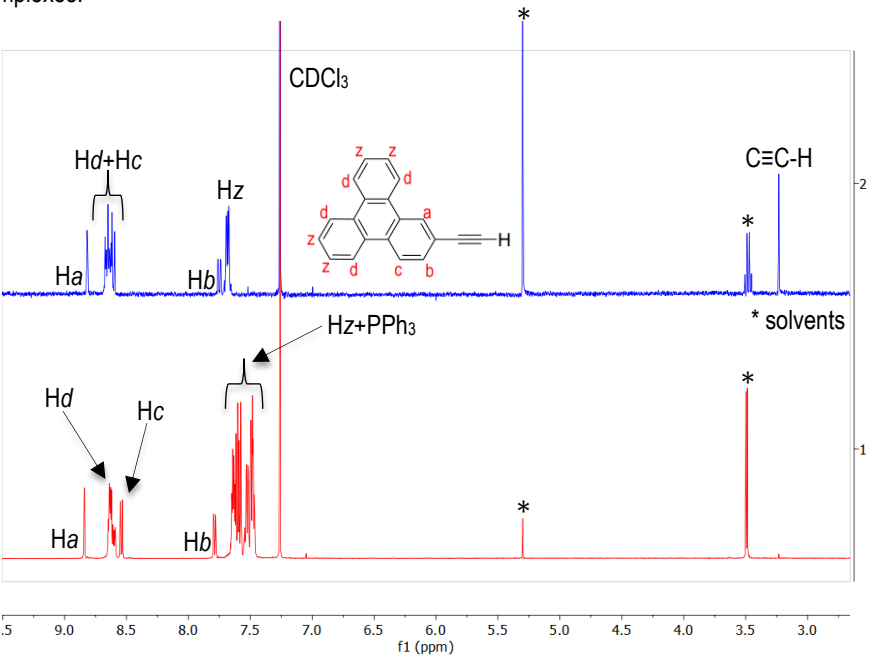

Figure 6. ^{1}H NMR (in $CDCl_3$) spectra of METP (up) and [METP-Au-PPh_3] (down) stacked.

Following the last procedure, the other gold(I) METP complexes containing other phosphine ligands have been synthesized, as it can be seen in scheme 3, and characterized through IR, ^{1}H NMR, ^{31}P NMR and mass spectrometry. In addition, the complex 4 was also analyzed through ^{13}C NMR, COSY and HSQC due to the complexity of its diastereotopic protons.

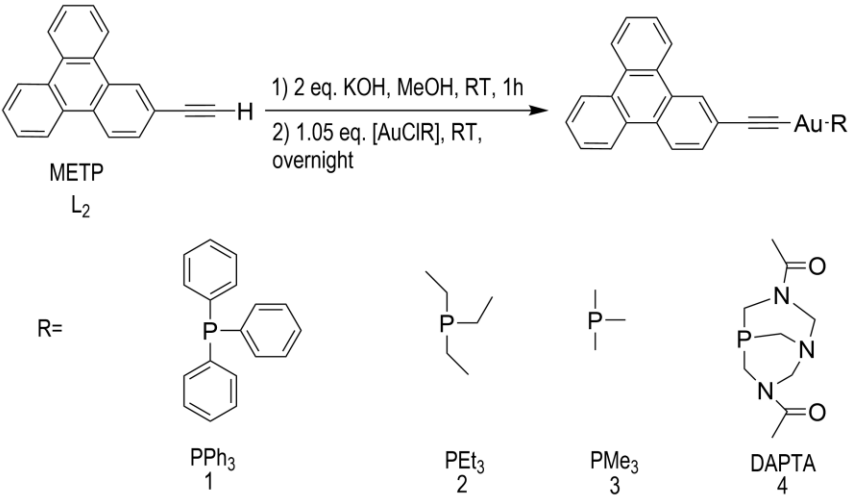

Scheme 3. Synthesis of [AuL_2R] (1-4) complexes.

Observing the IR spectra could be noticed if the peaks of the expected functional groups of the complexes were there. In the IR spectrum of [METP-Au-PEt_3], it could perfectly be observed the bending peaks of CH_2 and CH_3 at 1449 and 1379 cm^{-1} respectively, in addition to the Csp^3-H stretchings at 2966 and 2929 cm^{-1}. Furthermore, there were also the typical stretching peaks for all this complexes such as Csp^2-H, C=C Ar, C≡C, Ar ov. and bending =C-H op. as it can be seen in figure 7. Apart from those last peaks, at the [METP-Au-PMe_3] IR spectrum stood out the bending CH_3 peak at 1398 cm^{-1}. At the IR [METP-Au-DAPTA] spectrum, the only different peak from the others was the stretching C=O at 1637 cm^{-1}.

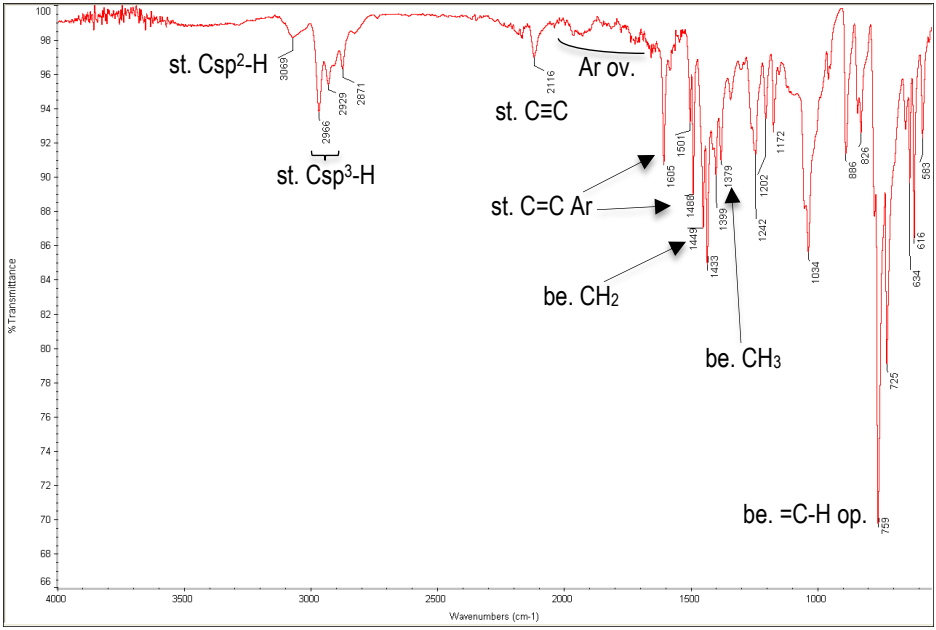

Figure 7. IR spectrum of [METP-Au-PEt$_3$].

Looking to the ^{1}H NMR spectra, the structures of the products were confirmed. In the ^{1}H NMR METP-Au-PEt$_3$ spectrum, it was observed that the protons *c* and *b* were overlapped with the multiplets of protons *d* and *z* respectively. Surprisingly, at 1.84 and 1.24 ppm appeared as broad singlets, the signals of P-$\underline{CH_2}$-CH_3 and P-CH_2-$\underline{CH_3}$ respectively. In the METP-Au-PMe$_3$ spectrum, the aromatic protons were not overlapped and could be appreciated the methyls signal as a doublet at 1.57 ppm as well as a doublet barely intense corresponding to the reactant [AuCl(PMe$_3$)]. To characterize the METP-Au-DAPTA and be able to assign each signal it was necessary to realize COSY (figure A1.2), HSQC and ^{13}C NMR spectra (figure A1.3) in addition to the ^{1}H NMR spectrum due to the large amount of diastereotopic protons of DAPTA. It was noticed that the methylenes between phosphorus and nitrogen appeared as a doublet of doublets (*e* and *f*) whereas the methylenes between two nitrogens appeared as a doublet (*g* and *h*), this is related to the greater proximity that the first ones have with the phosphorus, which they couple to. Surprisingly, it was noticed that the protons *i* were shown themselves as a singlet and were not diastereotopic. Furthermore, the *j* and *k* protons of the methyls appeared as two close, but different, singlets at 2.11 and 2.10 ppm. Finally, the aromatic protons followed the same way as in the

other spectra, without overlapping. In figure 8 is shown the area of the NMR spectrum of METP-Au-DAPTA between 5.9 and 3.5 ppm where the diastereotopic protons of the methylenes appear. The full spectrum is shown in figure A1.1.

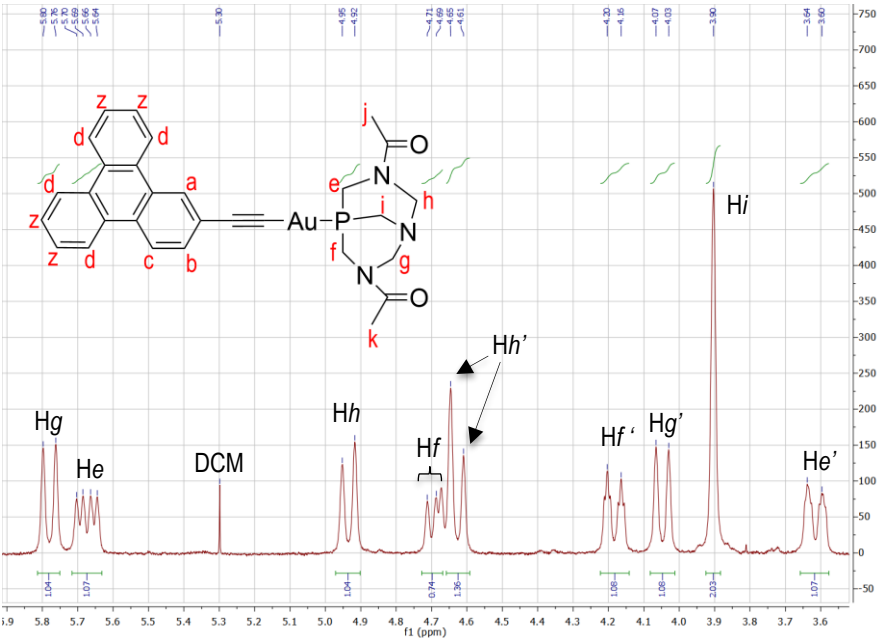

Figure 8. Expansion of ^{1}H NMR (in $CDCl_3$) spectrum of [METP-Au-DAPTA].

It could not be possible to assign all these protons in the ^{1}H NMR spectrum without the HSQC spectrum that is shown in figure 9, which relates the carbon with its corresponding proton. In the following figure is shown an expansion of the spectrum of the DAPTA area (with the exception of the methyls *j* and *k* that appear out of range). It can be appreciated that the carbons *e*, *f* and *i* appear as a doublet due to its greater proximity to the phosphorus and, thus, the coupling can be observed, whereas, in carbons *g* and *h* this coupling it is not visible. The full spectrum is shown in figure A1.4.

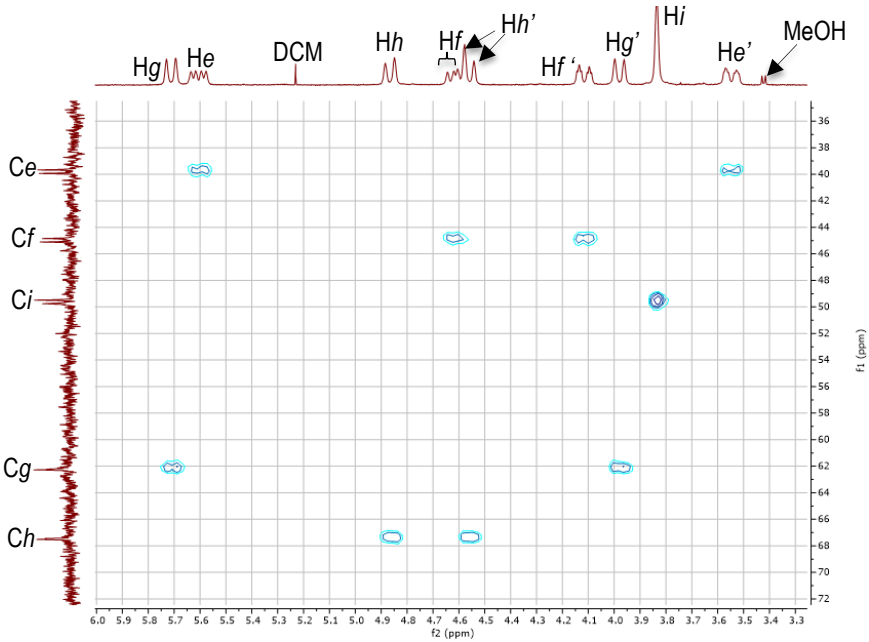

Figure 9. Expansion of HSQC (in $CDCl_3$) spectrum of METP-Au-DAPTA.

To continue, in the ^{31}P NMR spectrum of the [METP-Au-PEt_3] it was only observed one signal at 38.1 ppm that ensures the purity of the complex. On the other side, in the [METP-Au-DAPTA] spectrum could be noticed two signals, one small signal at 1.5 ppm and another one very intense at -22.1 ppm. These two signals in the ^{31}P NMR spectrum is common among DAPTA complexes and the intensity of them depends on the conformation of the complex among other factors. Moreover, in the [METP-Au-PMe_3] spectrum could be seen also two signals, one intense signal at -1.2 ppm corresponding to the complex and one small signal at -10.3 ppm according to the reactant [AuCl(PMe_3)].

Finally, it was required to look to the mass spectra of the compounds. At the [METP-Au-PEt_3] spectrum could be noticed the fragments $[M+H]^+$ and $[M+Na]^+$ at m/z 567.15 and 589.14 respectively. It also appeared a peak at 881.20 m/z corresponding to the fragment $[2M\text{-}METP]^+$. This type of peak was observed previously at the [METP-Au-PPh_3] spectrum and has become a typical fragment in these gold(I) METP complexes. On the other hand, the mass spectrum of the [METP-Au-DAPTA] was very fragmented and it could be only appreciated the fragments $[DAPTA+H]^+$ and $[DAPTA+Na]^+$.

6.1.4. Synthesis of HETP derivatives

Once the syntheses of METP derivatives were successfully accomplished, it was decided to start the syntheses of HETP derivatives adapting a synthetic method from the literature[5]. The complex using PMe_3 was not synthesized because the METP one was already very insoluble and trying it with HETP would only make a product really insoluble which would be impossible to characterize.

The first synthesis that was tried was the [HETP-(Au-PPh_3)$_6$]. Following the method mentioned before, the HETP was dissolved in MeOH and deprotonated with an excess of NaOH (10.5 eq.). The mixture was heated at reflux for 3 hours at 75°C, in order to make the HETP more soluble and help it react with NaOH. Past this time, the solution was allowed to cold at room temperature and 6.3 eq. of [AuCl(PPh_3)] were added and the mixture was stirred at 45°C over the weekend. On the next day, the solution was dried under vacuum, DCM was added and the mixture was filtrated trough cannula and both the crude and the filtrate were dried under vacuum. The products were characterized by IR and ^{1}H NMR and comparing the spectra with the HETP spectrum, it could be noticed that it must be some alkyne moieties without deprotonate. This was detected by looking into the IR and the ^{1}H NMR spectra, although the last one, the signal corresponding to C≡C-H appeared at the same chemical shift as the MeOH does, at 3.50 ppm. It also appeared the Csp-H peak at 3288 cm^{-1} at the IR spectrum.

With this acknowledgement, the reaction was repeated using KOH instead of NaOH and using more excess of base, around 12 eq. The heating after adding the gold(I) complex was also removed and the mixture was stirred overnight at room temperature. Doing so, an orange/brown powder was yielded and it was characterized through IR, ^{1}H NMR, ^{31}P NMR and mass spectrometry. Analyzing the spectra, it could be appreciated that the Csp-H peak at 3288 cm^{-1} at IR spectrum was disappeared but the signal at 3.50 ppm at the ^{1}H NMR spectra was still present either it was from MeOH or from some protonated alkynyl moiety. Moreover, the integrations of the aromatic protons of the ligand and from the PPh_3 were not the expected ones. The ^{31}P NMR also revealed that the peak of [AuCl(PPh_3)] unreacted at 33.2 ppm was greater than the peak corresponding to [HETP-(Au-PPh_3)$_6$] at 42.1 ppm. Finally, looking the mass spectrum it could be seen a very fragmented spectrum with the only significant peak at 721.15 corresponding to the [Au(PPh_3)$_2$]$^+$ fragment typical for all triphenylphosphine gold complexes.

Despite these problems, it was decided to try the syntheses of the other HETP derivatives to see if there were better achievements with more soluble compounds. The procedure to make these complexes was the same as the second try with [HETP-(Au-PPh_3)$_6$] as it can be seen in scheme 4.

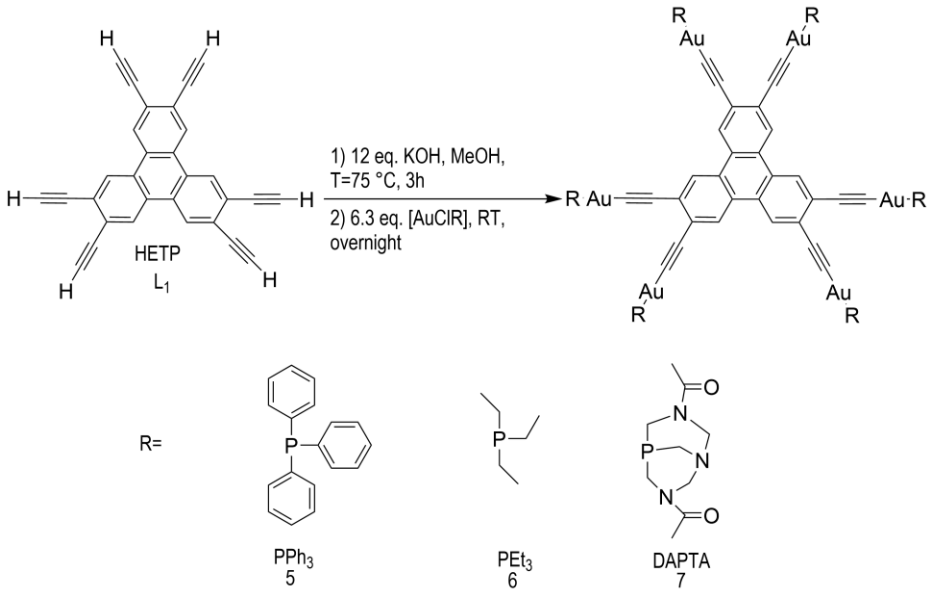

Scheme 4. Synthesis of [AuL_1R] (5-7) complexes.

The IR spectrum of the [HETP-(Au-PEt_3)$_6$] was not very clear, but some peaks could be appreciated such as the stretchings of Csp^2-H and Csp^3-H at 3099 and 2959 cm^{-1} respectively, and other peaks could be guessed such as the CH_2 and CH_3 bendings at 1488 and 1377 cm^{-1} respectively. Contrastingly, the IR spectrum of [HETP-(Au-DAPTA)$_6$] was recorded with better results. In the spectrum could be observed doubtless the stretching peaks corresponding to the Csp^3-H at 2959 and 2923 cm^{-1}, C≡C at 2110 cm^{-1} and C=O at 1633 cm^{-1}. Furthermore, it could be seen the bendings peaks according to CH_2, CH_3 and =C-H op. at 1412, 1331 and 791 cm^{-1} respectively.

Looking to the ^{1}H NMR spectra, the structures of the product were confirmed. In the ^{1}H NMR spectrum of [HETP-(Au-PEt_3)$_6$] it could perfectly be appreciated the aromatic protons

signal at 8.78 ppm that was appeared as a singlet. In addition, between 1.96-1.88 ppm it could be observed an overlapped double of quartets corresponding to the methylenes and between 1.13-1.05 ppm a double of triplets belonging to the methyls of the triethylphosphine as it can be seen in figure 10. These signals were noticed as a doublet of triplets or quadruplets due to the coupling between the protons and the phosphorus. In the ^{1}H NMR of [HETP-(Au-DAPTA)$_6$] (see figure A1.5), the signal of the aromatic protons was appeared slightly right-shifted at 8.71 ppm in relation to the [HETP-(Au-PEt$_3$)$_6$] signal. The signals of the diastereotopic protons of the DAPTA and the methyls followed the same patron as the [METP-Au-DAPTA] complex.

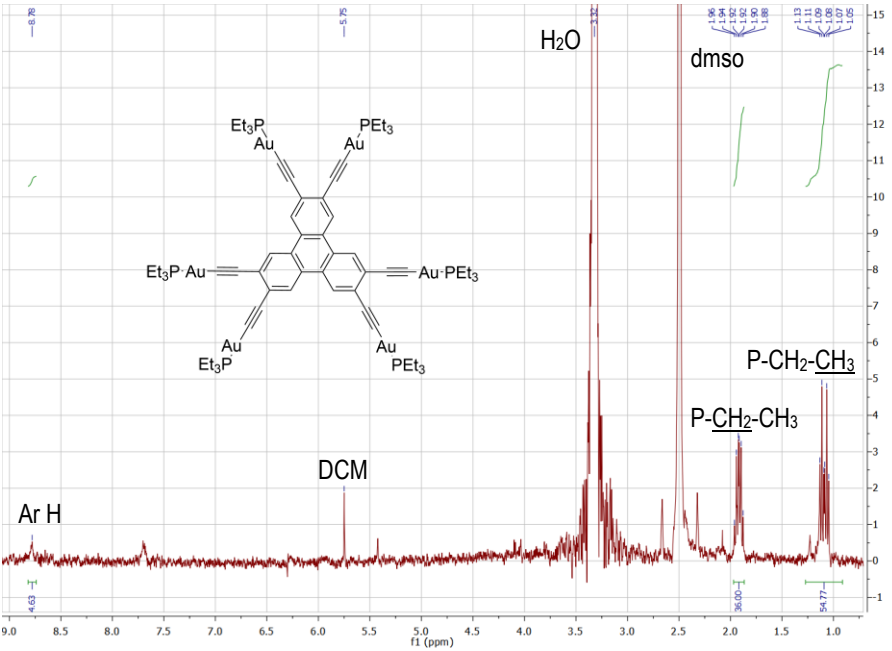

Figure 10. ^{1}H NMR (in dmso) spectrum of [HETP-(Au-PEt$_3$)$_6$].

To continue, in the ^{31}P NMR of [HETP-(Au-PEt$_3$)$_6$] it was only observed one signal at 33.85 ppm, which enhances the purity of the product. On the other hand, in the [HETP-(Au-DAPTA)$_6$] spectrum could be appreciated two signals as it happened with the [METP-Au-DAPTA] spectrum. One moderate intense signal was appeared at 1.5 ppm and one broad signal at -34.0 ppm. As it was commented before, the presence of two signals in DAPTA complexes is usual.

Lastly, by looking to the mass spectrum of [HETP-(Au-PEt$_3$)$_6$], its structure could be perfectly confirmed. It could be noticed the $[M+H]^+$ fragment at m/z 2259.2 and then, a group of

peaks that appeared with the losses of Au-PEt_3 moieties. These fragments can be observed in figure 11. In contrast, the mass spectrum of [HETP-(Au-DAPTA)$_6$] was very fragmented and any conclusions could not be made.

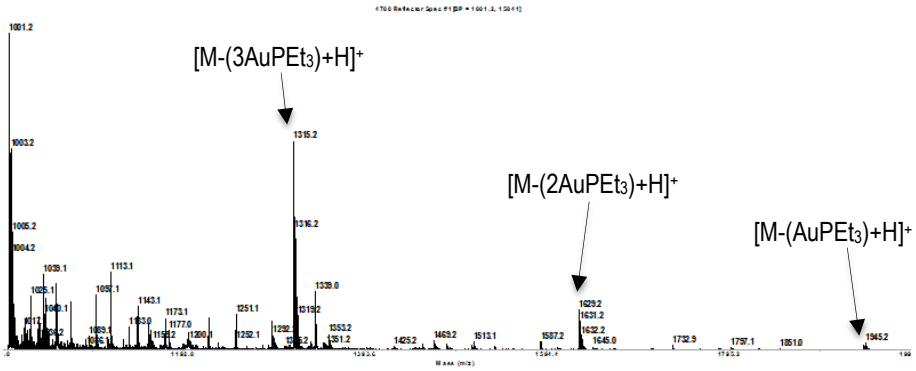

Figure 11. Expansion of [HETP-(Au-PEt_3)$_6$] mass spectrum.

6.2. LUMINESCENCE STUDIES

In this section, it was recorded at room temperature the absorption and emission spectra of some products earlier synthesized. The gold(I) complexes that were discarded for further studies were the [HETP-(AuPPh_3)$_6$], [METP-AuPPh_3] and [METP-AuPMe_3]. The first one, was not successfully achieved as it was commented before and the last two were not completely pure, so it was decided to focus on the triethylphosphine and DAPTA complexes.

In order to study the phosphorescence at room temperature it is required to record the emission spectra with the solutions being nitrogen saturated because the presence of oxygen is responsible for quenching the phosphorescence emission. Unlike other molecules, oxygen's ground state has a triplet spin and the two lowest energy excited electronic states of oxygen are singlet states. Energy transfer from a photoexcited molecule can induce the formation of singlet oxygen. This can be appreciated when singlet oxygen returns its triplet ground state and, therefore, it emits phosphorescence at 1270 nm[2]. This is showed in figure 12.

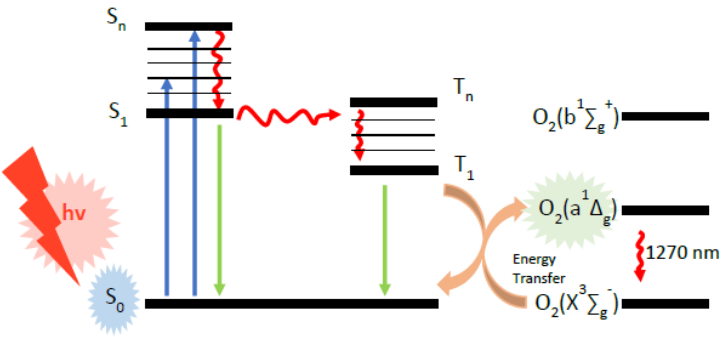

Figure 12. Singlet oxygen formation *(image extracted from Pinto, ref. 2)*.

6.2.1. Absorption and emission spectra of METP complexes

To record the absorption and emission spectra, solutions of the products in acetonitrile (ACN) were made. The concentration that was initially tried was $5 \cdot 10^{-5}$ M, but it was changed to $3 \cdot 10^{-5}$ M in order to obtain absorption maximums between 0.1 and 0.5 AU, thus, to be able to record successfully the emission spectra when excited. The results obtained are summarized in table 1.

Compound	Absorption λmax [nm] (ε[10^3 M^{-1} cm^{-1}])	Fluorescence emission λmax [nm] (with O_2)	Phosphorescence emission λmax [nm] (without O_2)
METP (L_2)	266 (66.9), 300 (13.3)	373	-
[METP-Au-PEt_3] (2)	266 (35.1), 323 (14.4)	377	479, 517
[METP-Au-DAPTA] (4)	276 (13.5), 323 (6.6)	378	481, 520

Table 1. Absorption and emission data from the gold(I) complexes 2 and 4, and the ligand precursor L_2 in ACN at RT. λ_{exc}=323 nm for 2 and 4; λ_{exc}=300 nm for L_2.

Both gold(I) complexes exhibit absorptions bands centered at *ca*. 270 and 323 nm as it can be seen in figure 13. These bands are red-shifted from the uncoordinated ligand due to the coordination to the gold atom, thus, they are assigned to an intraligand π⟶π*-(C≡C-R) or σ-(Au-P)⟶π*(C≡C-R) transition[8,14,15].

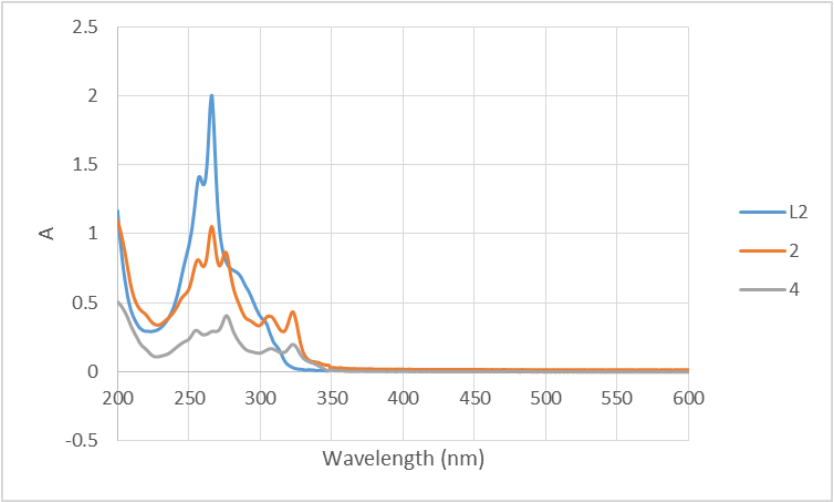

Figure 13. Absorption spectra in ACN of compounds L_2, 2 and 4 at $3 \cdot 10^{-5}$ M at RT.

In figure 14 can be observed the emission spectra of the complexes 2 and 4. It is noticed that the typical emission maxima for L_2 at 373 nm (see figure A2.1) is red-shifted when it is coordinated with the gold atom. These emission bands at *ca.* 375 nm are assigned to intraligand fluorescence transition[14].

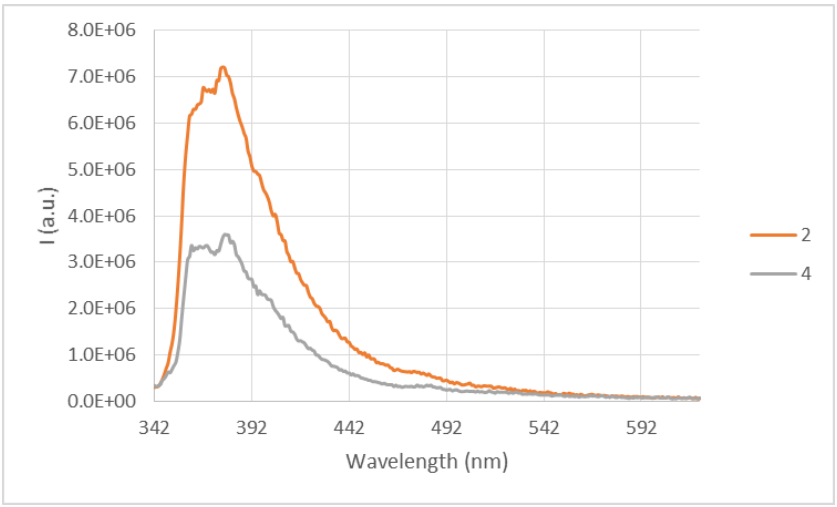

Figure 14. Emission spectra in ACN of compounds 2 and 4 at $3 \cdot 10^{-5}$ M at RT.

Finally, the emission spectra of the compounds were also recorded with the absence of oxygen in order to see if they presented phosphorescence. The spectrum of the precursor ligand L_2 remained invariable (see figure A2.2) whereas emission bands were appeared at *ca.* 480 and 520 nm for complexes 2 and 4, as it can be seen in figure 15. These bands are assigned to intraligand phosphorescence transitions[15].

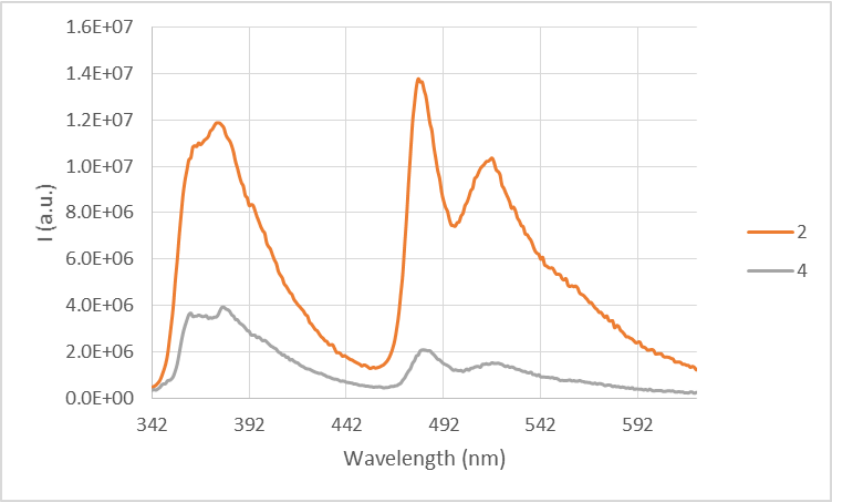

Figure 15. Emission spectra in ACN (without oxygen) of compounds 2 and 4 at $3 \cdot 10^{-5}$ M at RT.

The absence of phosphorescence bands in the ligand together with the appearance of these bands in the complexes confirms the enhancement of SOC by the presence of heavy atom that relaxes the spin selection rule and allows a fast ISC rate that favors the phosphorescence. It is hard to obtain room temperature phosphorescence, so the achievement of these levels of phosphorescence in these complexes are remarkable.

6.2.2. Absorption and emission spectra of HETP complexes

As it was mentioned before the hexa-substituted complexes were more insoluble than the mono-substituted complexes, therefore, after a first try where solutions of the products were made in ACN at a concentration of $3 \cdot 10^{-5}$ M, it was noticed that the compounds were not fully dissolved so it was decided to change the solvent to DCM. Moreover, the concentration of the solutions was also changed to $1.5 \cdot 10^{-5}$ M for the same reasons and to work in the range of 0.1-0.5 AU. It has to be mentioned that the noise that was appeared at *ca.* 240 nm, was originated by the cutoff of DCM. The results are summarized in table 2.

Compound	Absorption λmax [nm] (ε[10^3 M^{-1} cm^{-1}])	Fluorescence emission λmax [nm] (with O_2)	Phosphorescence emission λmax [nm] (without O_2)
HETP (L_1)	301 (90.9), 327 (28.7)	398, 420	-
[HETP-(Au-PEt_3)$_6$] (6)	339 (16.1), 362 (9.6)	420, 443	535, 584
[HETP-(Au-DAPTA)$_6$] (7)	301 (13.8), 326 (6.2)	398, 419	516, 560

Table 2. Absorption and emission data from the gold(I) complexes 6 and 7, and the ligand precursor L_1 in DCM at RT. λ_{exc}=327 nm for 7 and L_2; λ_{exc}=339 nm for 6.

The ligand L_1 and the complex 7 exhibit two absorption bands centered at *ca.* 300 and 327 nm. The first bands at a shorter wavelength are red-shifted from their monosubstituted resemblances and are assigned to an intraligand π⟶π*-(C≡C) or σ-(Au-P)⟶π*(C≡C) transition. On the other hand, the gold(I) complex 6 exhibits two absorption bands centered at *ca.* 340 and 360 nm which are strongly red-shifted from compounds L_1 and 7. The red-shift that complex 6 shows regarding ligand L_1 is greater than the red-shift that complex 2 exhibited regarding ligand L_2, this is due to the bigger coordination with gold atoms that complex 6 presents in front of complex 2. These bands are assigned to an intraligand π⟶π*-(C≡C-R) or σ-(Au-P)⟶π*(C≡C-R) transition and are also red-shifted from its mono-substituted resemblance[8,15,16]. This can be observed in figure 16.

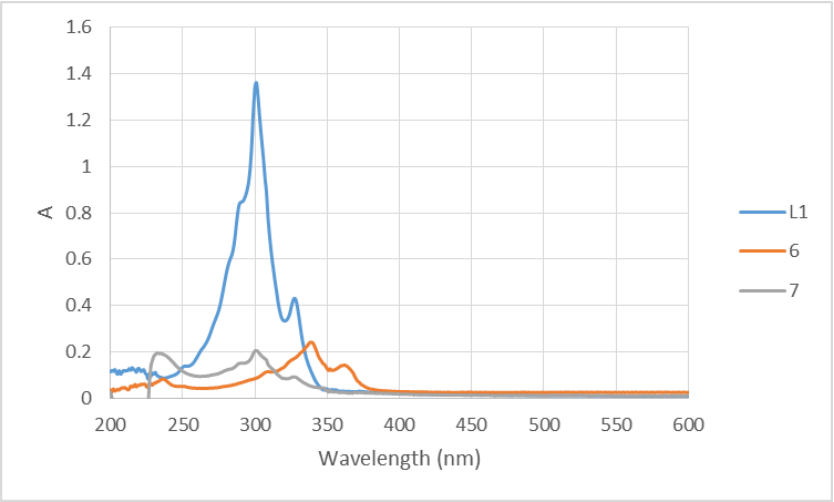

Figure 16. Absorption spectra in DCM of compounds L_1, 6 and 7 at $1.5 \cdot 10^{-5}$ M at RT.

In figure 17 can be observed the emission spectra of complexes 6 and 7. It is noticed that the complex 7 is not shifted regarding ligand L_1 that has the emission maximums at 398 and 420 nm (see figure A2.3), whereas compound 6 is *ca*. 20 nm red-shifted. These emission bands are assigned to intraligand fluorescence transitions. It is very remarkable that compound 6 presents two moderated phosphorescence bands centered at *ca.* 535 and 585 nm without the solution being nitrogen saturated because to our knowledge there are very few examples of compounds presenting phosphorescence in the presence of oxygen[14].

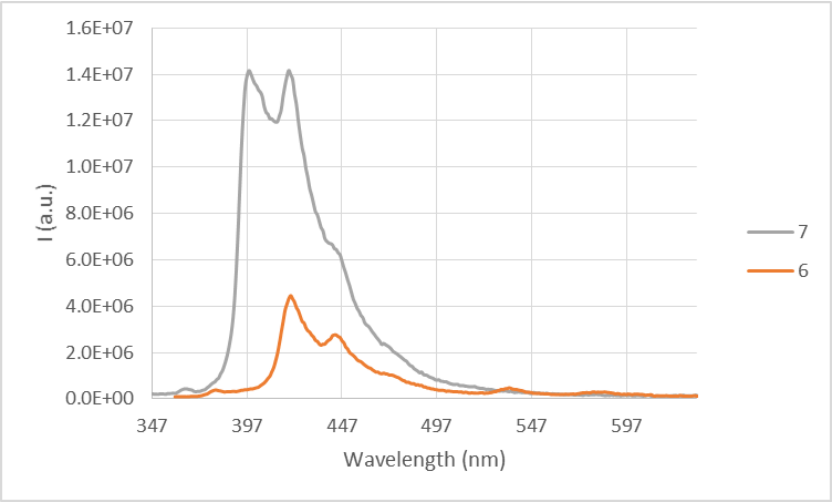

Figure 17. Emission spectra in DCM of compounds 6 and 7 at $1.5 \cdot 10^{-5}$ M at RT.

Finally, the emission spectra of the compounds were evaluated with the absence of oxygen in their solutions. The spectrum of the precursor ligand L_1 remained invariable (see figure A2.4) whereas in complexes 6 and 7 there was the appearance of two extra emission bands, this proves the phosphorescence inducing by adding gold(I) phosphane complexes to the uncoordinated ligand. Both complexes presented a red-shift regarding to their resemblance monosubstituted compounds (2 and 4), but this red-shift was bigger on the complex 6. These bands are assigned to intraligand phosphorescence transitions as it can be seen in figure 18.

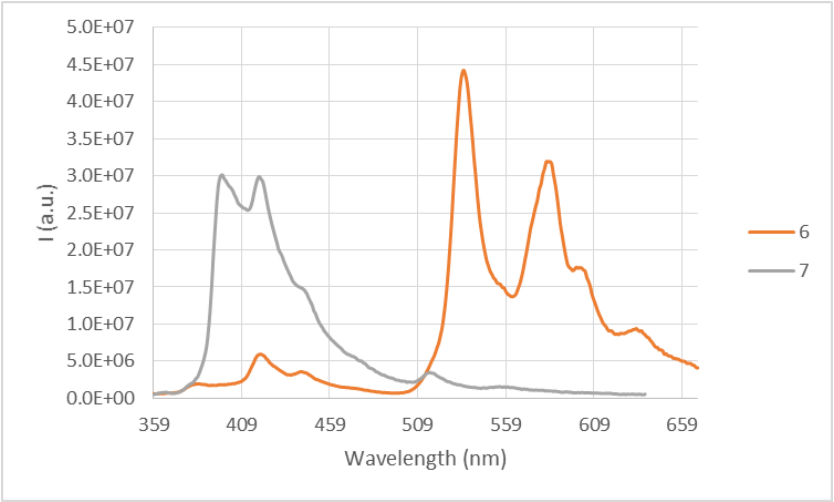

Figure 18. Emission spectra in DCM (without oxygen) of compounds 6 and 7 at $1.5 \cdot 10^{-5}$ M at RT.

The appearance of such intense phosphorescence bands at room temperature in the case of complex 6, where the phosphorescence dominates over the fluorescence, is an important achievement and could make it a very interesting candidate for further studies. The complex 7 also presented two phosphorescence bands centered at *ca.* 516 and 560 nm at room temperature but at lower intensities.

7. CONCLUSIONS

Looking at the obtained results, it can be confirmed that Sonogashira cross coupling is an efficient method to prepare alkynyl ligands such as HETP. Moreover, it is observed that using a less hygroscopic base such as KOH is better than NaOH for the deprotonation of both METP and HETP.

The synthesis of the gold(I) complexes showed that the synthetic pathway was successful for most of the compounds and the principal issue was the insolubility of the hexasubstituted complexes and [METP-Au-PMe_3].

The achievement of these reactions was confirmed by IR, ^{1}H and ^{31}P NMR and mass spectrometry. In the case of both DAPTA complexes, additional techniques were required to characterize the compounds such as ^{13}C NMR, COSY and HSQC.

The luminescence studies showed that by adding the gold(I) phosphane complexes to the ligands, the emission fluorescence maximums were diminished due to the presence of the gold atom that enhances SOC, which relaxes the spin selection rule and allows a fast ISC rate that favors the population of the triplet state. This greater population of the triplet state is what allows the appearance of phosphorescence. The luminescence is due to intraligand $\pi \rightarrow \pi^*$-(C≡C-R) or σ-(Au-P)$\rightarrow \pi^*$(C≡C-R) transitions. The luminescence results of the analyzed compounds are so positive showing everyone room temperature phosphorescence in the absence of oxygen. The case of complex 6, [HETP-(Au-PEt_3)$_6$], is especially interesting because it presented room temperature phosphorescence with the presence of oxygen, and when the solution was nitrogen saturated, the phosphorescence bands were far more intense than the fluorescence bands. That makes [HETP-(Au-PEt_3)$_6$] an ideal candidate for further studies and applications such as OLEDs, chemical sensor or bioimaging probes.

8. REFERENCES AND NOTES

1. He, X. Luminescent gold(I) complexes for chemosensing. *Coord. Chem. Rev.* **255**, 2111–2123 (2011).
2. Pinto, A. Luminescent gold(I) supramolecular assemblies on materials and biological chemistry (Doctoral thesis). (Universitat de Barcelona, 2021).
3. Obodovskiy, I. *Luminescence*. *Radiation* (Elsevier, 2019).
4. Schulman, S. G. *Fluorescence and Phosphorescence Spectroscopy: Physicochemical principles and practice*. *Spectroscopy* (Pergamon, 1977).
5. Gutiérrez-Blanco, A., Fernández-Moreira, V., Gimeno, M. C., Peris, E. & Poyatos, M. Tetra-Au(I) Complexes Bearing a Pyrene Tetraalkynyl Connector Behave as Fluorescence Torches. *Organometallics* **37**, 1795–1800 (2018).
6. Caparrós, F. J., Outis, M., Jung, Y., Choi, H., Lima, J. C., & Rodríguez, L. Luminescent tetranuclear gold(I) dibenzo[g,p]chrysene derivatives: Effect of the environment on photophysical properties. *Molecules* **25**, 949–960 (2020).
7. Runeberg, N., Schütz, M. & Werner, H. J. The aurophilic attraction as interpreted by local correlation methods. *J. Chem. Phys.* **110**, 7210–7215 (1999).
8. Pujadas, M. & Rodríguez, L. Luminescent phosphine gold(I) alkynyl complexes. Highlights from 2010 to 2018. *Coord. Chem. Rev.* **408**, 213179, (2020).
9. Martinez, C. R. Rethinking the term 'pi-stacking'. *Chem. Sci.* **3**, 2191–2201 (2012).
10. Moro, A. J. A coumarin based gold(I)-alkynyl complex: a new class of supramolecular hydrogelators. *Org. Biomol. Chem.* **13**, 2026–2033 (2015).
11. Ferrer, M., Gutiérrez, A., Rodríguez, L., Rossell, O., Lima. J. C., Font-Bardia, M. & Solans, X. Study of the effect of the phosphane bridging chain nature on the structural and photophysical properties of a series of gold(I) ethynylpyridine complexes. *Eur. J. Inorg. Chem.* **3**, 2899–2909 (2008).
12. Ye, X. L., Huang, Y. Q., Tang, X. Y., Xu, J., Peng, C., & Tan, Y. Z. Two-dimensional extended π-conjugated triphenylene-core covalent organic polymer. *J. Mater. Chem. A* **7**, 3066–3071 (2019).
13. Schilz, M. & Plenio, H. A guide to sonogashira cross-coupling reactions: The influence of substituents in aryl bromides, acetylenes, and phosphines. *J. Org. Chem.* **77**, 2798–2807 (2012).
14. de Aquino, A., Caparrós, F. J., Truong, K. N., Rissanen, K., Ferrer, M., Jung, Y., Choi, H., Lima, J. C. & Rodríguez, L. Gold(i)-doped films: new routes for efficient room temperature phosphorescent materials. *Dalton Trans.* **50**, 3806–3815 (2021).
15. de Aquino, A., Caparrós, J. C., Aullón, G., Ward, J. S., Rissanen, K., Jung, Y., Choi, H., Lima, J. C., Rodríguez, L. Effect of Gold(I) on the Room-Temperature Phosphorescence of Ethynylphenanthrene. *Chemistry - A European Journal* **27**, 1810–1820 (2021).
16. Rosental, M., Coldman, R. N., Moro, A. J., Angurell, I., Gomila, R. M., Frontera, A., Lima, J. C., Rodríguez, L. Using room temperature phosphorescence of gold(I) complexes for pahs sensing. *Molecules* **26**, 2444-2458 (2021).

9. ACRONYMS

Triphenylene	TP
2,3,6,7,10,11-hexabromotriphenylene	HBTP
Hexa(trimethylsilylethynyl)triphenylene	HTMSTP
2,3,6,7,10,11-hexaethynyltriphenylene	HETP
Aromatic	Ar
2-ethynyl-triphenylene	METP
Room Temperature	RT
1,1'-(1,3,7-Triaza-5-phosphabicyclo[3.3.1]nonane-3,7-diyl)diethanone	DAPTA
Equivalent	eq.
Retention factor	Rf
Majority	maj.
Minority	min.
Dimethyl sulfoxide	dmso
Circa.	*ca.*

APPENDICES

APPENDIX 1: CHARACTERIZATION SPECTRA OF DAPTA COMPLEXES

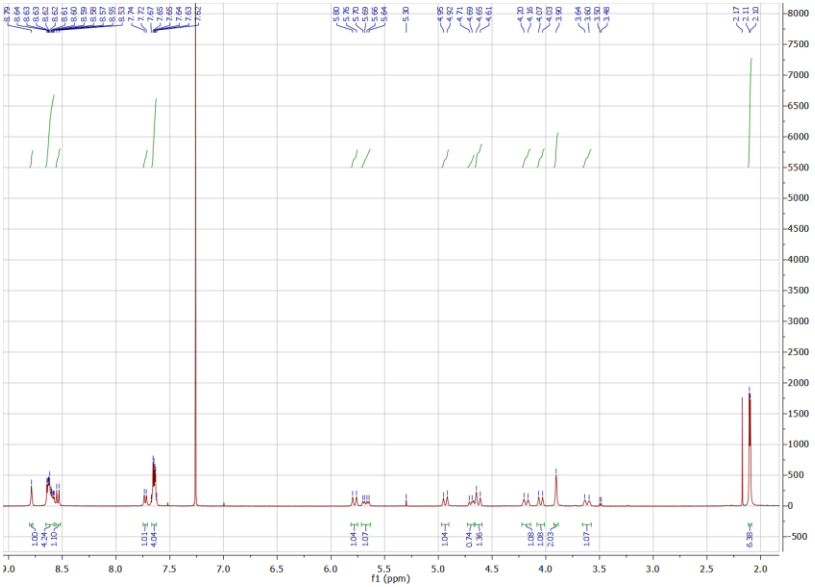

Figure A1.1. ^{1}H NMR (in $CDCl_3$) spectrum of [METP-Au-DAPTA].

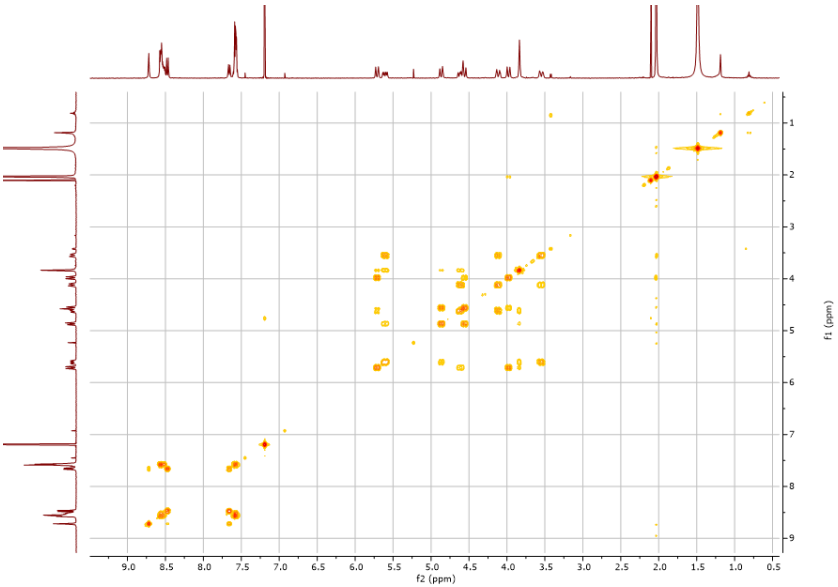

Figure A1.2. COSY (in $CDCl_3$) spectrum of [METP-Au-DAPTA].

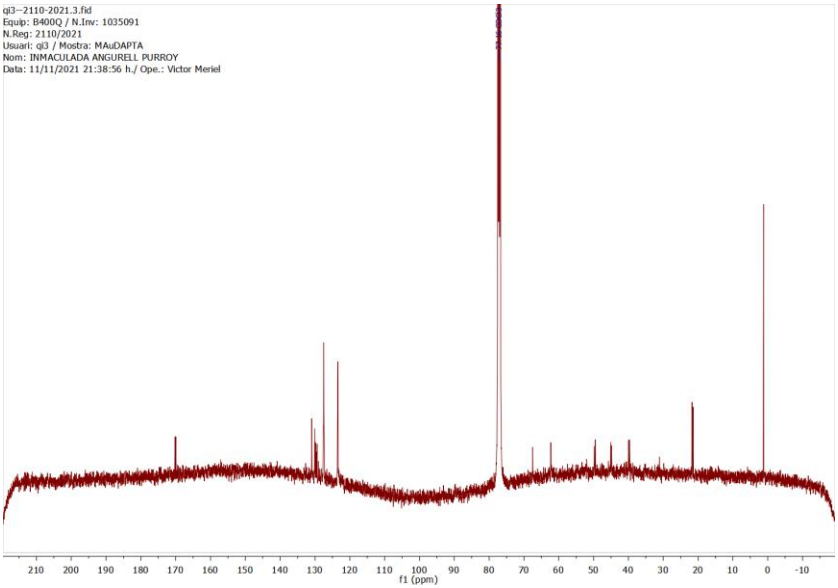

Figure A1.3. ^{13}C NMR (in $CDCl_3$) spectrum of [METP-Au-DAPTA].

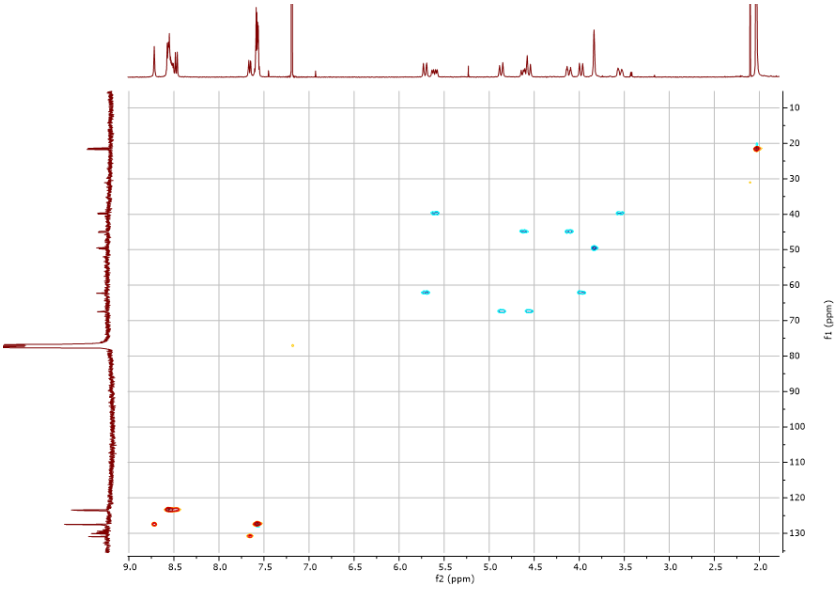

Figure A1.4. HSQC (in $CDCl_3$) spectrum of [METP-Au-DAPTA].

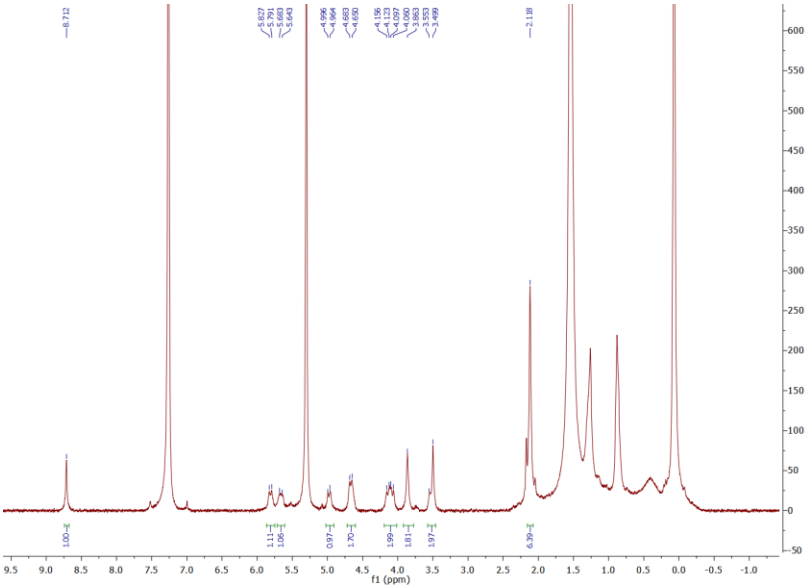

Figure A1.5. ^{1}H NMR (in $CDCl_3$) spectrum of [HETP-(Au-DAPTA)$_6$].

APPENDIX 2: LIGANDS EMISSION SPECTRA

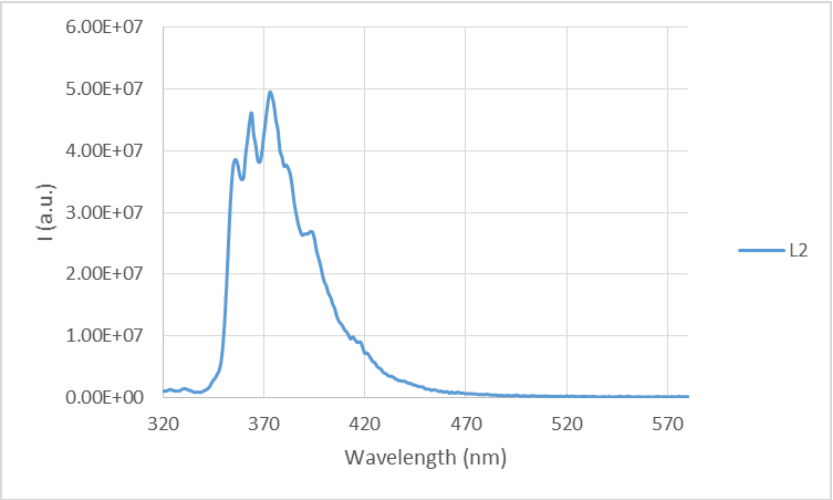

Figure A2.1. Emission spectrum in ACN of METP at $3 \cdot 10^{-5}$ M at RT.

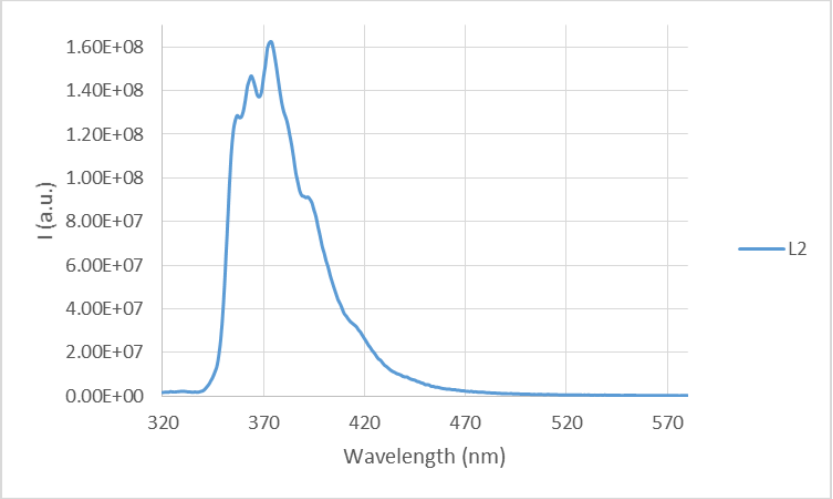

Figure A2.2. Emission spectrum in ACN (without oxygen) of METP at $3 \cdot 10^{-5}$ M at RT.

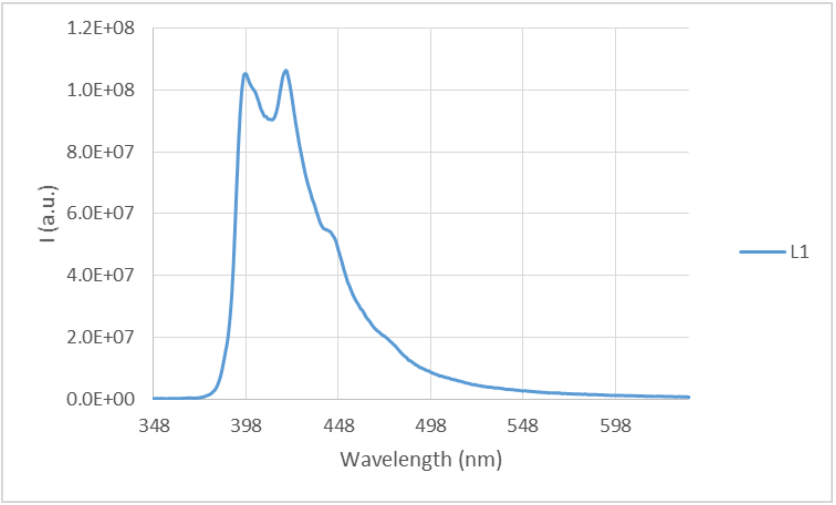

Figure A2.3. Emission spectrum in DCM of HETP at $1.5 \cdot 10^{-5}$ M at RT.

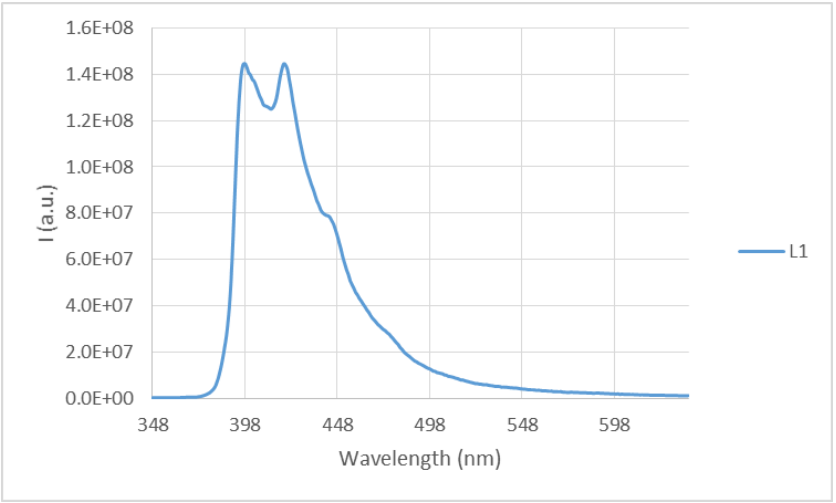

Figure A2.4 Emission spectrum in DCM (without oxygen) of HETP at $1.5 \cdot 10^{-5}$ M at RT.